

## TEMPERATURE AND PRECIPITATION VARIABILITY IN THE EUROPEAN ALPS SINCE 1500

CARLO CASTY,<sup>a,b,\*</sup> HEINZ WANNER,<sup>b</sup> JÜRIG LUTERBACHER,<sup>b</sup> JAN ESPER<sup>c</sup> and REINHARD BÖHM<sup>d</sup>

<sup>a</sup> *Climate and Environmental Physics, Physics Institute, University of Bern, Sidlerstrasse 5, CH-3012 Bern, Switzerland*

<sup>b</sup> *Institute of Geography and NCCR Climate, University of Bern, Switzerland*

<sup>c</sup> *Swiss Federal Research Institute WSL, CH-8903 Birmensdorf, Switzerland*

<sup>d</sup> *ZAMG – Central Institute for Meteorology and Geodynamics, Vienna, Austria*

*Received 30 July 2004*

*Revised 13 May 2005*

*Accepted 13 May 2005*

### ABSTRACT

High-resolution temperature and precipitation variations and their seasonal extremes since 1500 are presented for the European Alps (43.25–48.25°N and 4.25–16.25°E). The spatial resolution of the gridded reconstruction is given by 0.5° × 0.5° and monthly (seasonal) grids are reconstructed back to 1659 (1500–1658). The reconstructions are based on a combination of long instrumental station data and documentary proxy evidence applying principal component regression analysis. Annual, winter and summer Alpine temperatures indicate a transition from cold conditions prior to 1900 to present day warmth. Very harsh winters occurred at the turn of the seventeenth century. Warm summers were recorded around 1550, during the second half of the eighteenth century and towards the end of the twentieth century. The years 1994, 2000, 2002, and particularly 2003 were the warmest since 1500. Unlike temperature, precipitation variation over the European Alps showed no significant low-frequency trend and increased uncertainty back to 1500. The years 1540, 1921 and 2003 were very likely the driest in the context of the last 500 years.

Running correlations between the North Atlantic Oscillation Index (NAOI) and the Alpine temperature and precipitation reconstructions demonstrate the importance of this mode in explaining Alpine winter climate over the last centuries. Winter NAOI correlates positively with Alpine temperatures and negatively with precipitation. These correlations, however, are temporally unstable. We conclude that the Alps are situated in a band of varying influence of the NAO, and that other atmospheric circulation modes controlled Alpine temperature and precipitation variability through the recent past. Copyright © 2005 Royal Meteorological Society.

KEY WORDS: European Alps; principal component regression; temperature; precipitation; climate variability; reconstructions; North Atlantic Oscillation

### 1. INTRODUCTION

Improved understanding of long-term, natural climate variability on different spatio-temporal scales is crucial to place the recent, potentially anomalous, changes in a longer term context (e.g. Jones and Mann, 2004 and references therein; Luterbacher *et al.*, 2004; Moberg *et al.*, 2005). It is therefore important to extend existing climatic records, such as temperature, precipitation, and circulation patterns, as far back in time as possible (e.g. Jones *et al.*, 2001). A number of previous studies have focused on global to hemispheric temperature reconstructions over the past few centuries to millennia, based on both empirical proxy data (Bradley and Jones, 1993; Overpeck *et al.*, 1997; Jones *et al.*, 1998; Mann *et al.*, 1998, 1999; Crowley and Lowery, 2000; Briffa *et al.*, 1998, 2001, 2002, 2004; Esper *et al.*, 2002; Cook *et al.*, 2004; Huang, 2004; Pollack and Smerdon, 2004; Moberg *et al.*, 2005; Oerlemans, 2005) and model simulations including forcing data (e.g. Crowley, 2000; Bauer *et al.*, 2003; Gerber *et al.*, 2003; González-Rouco *et al.*, 2003; Rutherford *et al.*, 2003,

\*Correspondence to: Carlo Casty, Climate and Environmental Physics, Physics Institute, Sidlerstrasse 5, CH-3012 Bern, Switzerland; e-mail: casty@climate.unibe.ch

2005; von Storch *et al.*, 2004; Goosse *et al.*, 2005a,b). Several of these temperature reconstructions conclude that late twentieth-century warmth is unprecedented at hemispheric scales, and can only be explained by anthropogenic, greenhouse gas forcing (Jones and Mann, 2004, and references therein).

Hemispheric temperature reconstructions, however, provide little information about regional-scale climate variations. Several sources point to differing courses of temperature change in Europe, and a greater amplitude of variations than recorded for the Northern Hemisphere (e.g. Mann *et al.*, 2000; Luterbacher *et al.*, 2004; Jones and Mann, 2004; Brázdil *et al.*, 2005; Guiot *et al.*, 2005; Xoplaki *et al.*, 2005). For example, the hot European summer of 2003 was a regional expression of an extreme event, much larger in amplitude than extremes at hemispheric scales (Chuine *et al.*, 2004; Luterbacher *et al.*, 2004; Pal *et al.*, 2004; Rebetz, 2004; Schär *et al.*, 2004; Schönwiese *et al.*, 2004; Stott *et al.*, 2004; Menzel, 2005). That summer had a significant regional impact on environment, society and economy (Koppe *et al.*, 2004; Kovats *et al.*, 2004; Kovats and Koppe, 2005; Stèphan *et al.*, 2005; Valleron and Boumendil, 2004).

The European Alps are a 200 km wide and 800 km long mountain range extending from about 44 to 48°N and 3 to 16.5°E. Its highest peaks reach 4400 to 4800 m a.s.l., and its average elevation is ~2500 m. North Atlantic weather systems, the Mediterranean Sea and the large Eurasian land mass influence climate variability in the European Alps (Wanner *et al.*, 1997; Böhm *et al.*, 2001; Beniston and Jungo, 2002; Begert *et al.*, 2005; Auer *et al.*, 2005). The North Atlantic Oscillation (NAO; e.g. Wanner *et al.*, 2001; Hurrell *et al.*, 2003 and references therein) is the dominant climate mode for Europe, particularly controlling the weather patterns in western and northern Europe (Auer *et al.*, 2001a). However, the Alps are situated in a band between northern and southern Europe, where the forcing of the NAO is amplified with distance north and south of the Alpine area (Beniston *et al.*, 1994; Beniston and Jungo, 2002).

Here we present high-resolution reconstructions of gridded temperature and precipitation patterns for the greater European Alpine region back to 1500 using long instrumental data in combination with documentary proxy evidence. The reconstructions cover the area 43.25–48.25°N and 4.25–16.25°E (excluding non-alpine parts in France, the Po Plain and Croatia) with a spatial resolution of 0.5° × 0.5° equal to 199 grid points and complement recently established tree-ring based reconstructions over the European Alps or parts of it (e.g. Frank and Esper, 2005; Büntgen *et al.*, 2005; Wilson *et al.*, 2005).

In Section 2, the data and methods are explained. Section 3 presents the annual, winter and summer means of temperature and precipitation variability for all grid points representing the European Alps. We add uncertainty intervals to these reconstructions, and derive the coldest and wettest winters (DJF) as well as the warmest and driest summers (JJA) in the 1500–1900 reconstruction period, and assess the reconstruction quality of these extremes. Extended winter temperature and precipitation time series are then related to the North Atlantic Oscillation Index (NAOI), independently reconstructed using tree-ring and ice core data (Cook *et al.*, 2002) to investigate the influence of this mode on Alpine climate since 1659. The discussion and conclusions are given in Sections 4 and 5.

## 2. DATA AND METHODS

Eighty seven early instrumental temperature and 146 precipitation time series from all over Europe (Auer *et al.*, 2001a,b, 2005; Böhm *et al.*, 2001; Luterbacher *et al.*, 2002a,b, 2004; Begert *et al.*, 2005) in combination with 11 (12) documentary records for temperature (precipitation) including estimates derived from narratives, annals, scientific writings and monastery records (Brázdil *et al.*, 2005 and references therein) are used as predictors for the gridded reconstruction of the greater Alpine area climate (Figures 1(a),(b)). The data detailed by Mitchell *et al.* (2004; CRU TS 2.0; [http://www.cru.uea.ac.uk/~timm/grid/CRU\\_TS\\_2\\_0.html](http://www.cru.uea.ac.uk/~timm/grid/CRU_TS_2_0.html)), comprising monthly global land surface grids of observed climate for the 1901–2000 period with 0.5° resolution (~60 km × 60 km), serve as predictands. These data revise and extend the recently published version of New *et al.* (2000). We selected the 199 grid points representing the greater Alpine area (43.25–48.25°N and 4.25–16.25°E), excluding non-alpine parts in France (46.25–48.25°N and 4.25–5.75°E), the Po Plain and Croatia (43.25–45.25°N and 5.75–16.25°E).

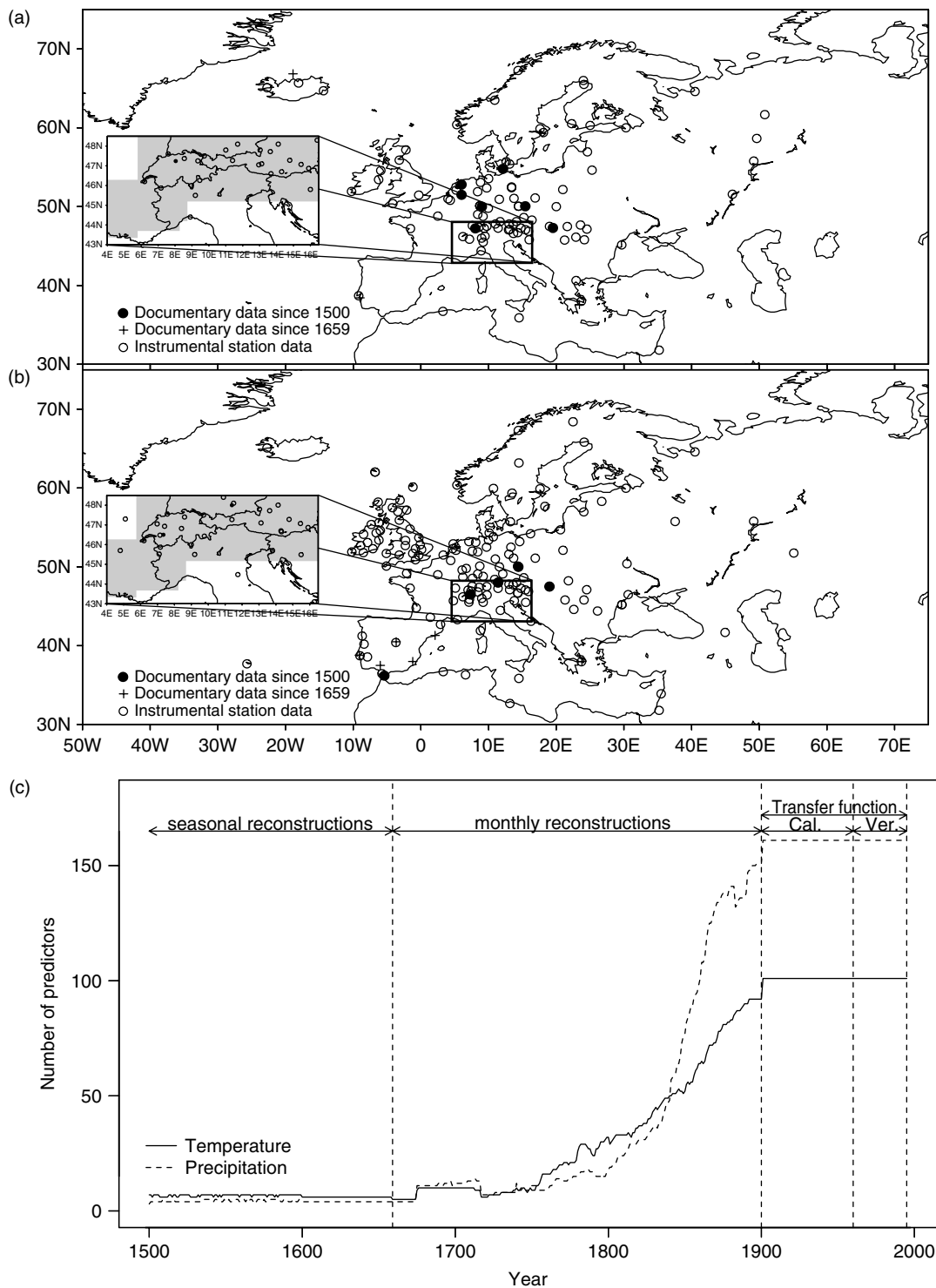


Figure 1. (a) Spatial distribution of the predictor data for the Alpine temperature reconstructions. The grey shading in the small box plot in the enlarged sector reveals the reconstructed Alpine area. (b) same as (a) but for the predictor data for the Alpine precipitation reconstruction. (c) The temporal evolution of the number of predictors for temperature (solid line) and precipitation (dotted line)

Temperature and precipitation are reconstructed independently, i.e. they share no common predictors. Figure 1(c) shows the temporal evolution of the predictors from 1500 to the late twentieth century. From 1500 to 1658, only 11 (12) indices for temperature (precipitation) are available. The instrumental station number increases steadily from 1750 onward. In the twentieth century, a maximum of 98 temperature predictors and 158 precipitation predictors are used (see also Appendices 1 and 2).

Alpine near surface air temperature and precipitation patterns are reconstructed with monthly resolution back to 1659 and seasonal back to 1500, using principal component regression as outlined in Luterbacher *et al.* (2004). First, the leading Empirical Orthogonal Functions (EOFs) accounting for 90% of the predictor data variance and the leading EOFs explaining 95% of the total predictand variability (gridded temperature and precipitation, respectively, Mitchell *et al.*, 2004) are calculated for the 1901–1960 calibration period. A multivariate regression is then performed against each of the grid point EOFs of the calibration period against all the retained EOFs of the predictor data. Applying the multivariate regression model to independent data from the 1961–1995 verification period allows testing the performance of the reconstructions. Owing to the changing number of the predictor data over time (Figure 1(c)), 10 nested models for the 1500–1658 period are developed for temperature (12 for precipitation) and 390 for the 1659 period onwards (458 for precipitation).

Averaging all 199 grid points over the European Alpine region allows regional time series of temperature and precipitation to be derived with the unresolved variance in the regression (Standard error, SE; e.g. von Storch and Zwiers, 2001; Briffa *et al.*, 2002) as uncertainty estimates. The new reconstructions are then compared with the predictor CRU data (Mitchell *et al.*, 2004) over the verification period, grid point by grid point, for the entire study area. The Reduction of Error statistic (RE, see Cook *et al.*, 1994 for a review) is used to estimate the strength of the linear relationship between reconstruction and observation. RE is the expected fraction of the predictand variance, given by the predictor. It ranges from  $-\infty$  to  $+1$  with a zero value indicating the skill of climatological means and increasingly positive RE indicating increased regression skill.  $RE + 1$  would be a perfect reconstruction, whereas  $-1 < RE < 0$  is better than random. We performed several sensitivity experiments in order to maximize RE statistics over time. It turned out that 80% (90%) of the explained variance of the predictor data and for temperature (precipitation) and 80% (95%) of the predictand CRU data (Mitchell *et al.*, 2004) returned the most useful results (not shown). Finally, we recalibrated over the 1901–1995 period in order to derive the final temperature and precipitation patterns for the 1500–1900 period for the Alpine area.

From 1901 to 2000 we used the temperature and precipitation data by Mitchell *et al.* (2004). The post-2000 temperature data is an update from (Hansen *et al.* 1999, 2001). The precipitation data from 2001 to 2003 (2001 to 2004 for winter) is the CPC Merged Analysis of Precipitation (CMAP)  $2.5^\circ \times 2.5^\circ$  grid for the Alpine region (Xie and Arkin, 1997, updated). These monthly data span the 1979 period onward. The correlation between the CRU and the CMAP monthly precipitation data is 0.95 for the 1979–2000 period and no significant bias is detected (not shown). Therefore, in order to calculate the anomalies for the CMAP data with regard to the twentieth-century mean, the 1901–2000 CRU precipitation data are interpolated on the  $2.5^\circ \times 2.5^\circ$  CMAP grid, and the twentieth-century monthly means of the interpolated CRU data are subtracted from the corresponding CMAP data.

We use 31-year running Pearson (Spearman) correlations to study the temporal relationship between the extended winter (DJFM) temperature (precipitation) time series and winter NAOI reconstruction by Cook *et al.* (2002). These data are independent of the reconstruction presented in this study; i.e. they do not share predictor data. Gershunov *et al.* (2001) state that significant correlations can occur only from random processes and do not have to be physically meaningful. Therefore, to better evaluate the signal-to-noise ratio of the obtained running correlation coefficients we estimated 95% confidence levels using a Monte Carlo simulation. One thousand random time series having the same standard deviation, mean and lag-one autocorrelation coefficients as the original ones are computed and then correlated with the NAOI (Wilks, 1995).

### 3. RESULTS

#### 3.1. Alpine temperature variability 1500–2003

Figure 2 shows the average annual, winter (DJF) and summer (JJA) temperature anomalies for the Alps with regard to the 1901–2000 mean. Extremes are defined as values exceeding  $\pm 2$  standard deviations of the twentieth century. The numbers mark extremes within the reconstruction for the period prior to 1900. The annual Alpine mean reveals that the 1590s, 1690s, 1730s and 1890s were harsh (Figure 2(a)). Warm periods are distinguished from about 1780 to 1810, 1890 to 1945, and the 1970s onward. The accumulation of positive temperature extremes during the last 10 years is remarkable. In the Alpine area, 1994, 2000, 2002 and 2003 were the warmest within the last 500 years. 1540 was the warmest year ( $+1.4^{\circ}\text{C}$  compared with the twentieth century annual Alpine mean temperature of  $8^{\circ}\text{C}$ ) and 1740 the coldest year during the reconstruction period ( $-2.5^{\circ}\text{C}$ ). Table I presents all extremes as derived from the annual, winter, and summer time series by exceeding the two standard deviations of the 1901–2000 period. The uncertainties of the reconstruction are  $\sim 0.85^{\circ}\text{C}$  from 1500 to 1770 and  $0.2^{\circ}\text{C}$  from the nineteenth century to the present.

The pre-1900 winter temperatures (Figure 2(b)) were generally colder than those of the twentieth century. The lowest temperatures were recorded during the last decades of the seventeenth century, which is in agreement with the coldest period over Europe back to 1500 (Luterbacher *et al.*, 2001, 2004; Xoplaki *et al.*, 2005). Winters in the 1690s were extremely harsh in the Alpine area with temperature anomalies of  $-1.6^{\circ}\text{C}$  in agreement with independent findings of Pfister (1992, 1999). Shorter cold periods appear in the sixteenth century and around 1890. A strong transition to warm winter conditions is found from 1890 to 1915. After the 1960 winter, Alpine temperatures were above the average twentieth-century conditions. With an anomaly of  $-4.8^{\circ}\text{C}$ , 1829/1830 was the coldest Alpine winter (twentieth century winter mean temperature is  $0^{\circ}\text{C}$ ) and 1606/1607 the warmest ( $+3.5^{\circ}\text{C}$ ). The uncertainties of the winter reconstruction are  $\sim 1.1^{\circ}\text{C}$  until 1770 and  $\sim 0.6^{\circ}\text{C}$  since the nineteenth century.

Figure 2(c) presents the Alpine summer temperature variability between 1500 and 2003. The variability is lower for summer than for winters. Warm summers were experienced around 1550, periodically in the seventeenth century, in the second half of the eighteenth century, from 1946 to 1950 and from 1970 onward. The summer of 2003 was by far the warmest since 1500 with a unique anomaly of around  $+4.4^{\circ}\text{C}$  compared with the summer mean temperature 1901–2000 of  $16.1^{\circ}\text{C}$ . 1807 was the warmest Alpine summer during the reconstruction period ( $+2.15^{\circ}\text{C}$ ). The absolute coldest Alpine summer was 1816 ( $-1.9^{\circ}\text{C}$ ), in agreement with the findings of Pfister (1992, 1999). The uncertainties of the reconstruction are  $0.6^{\circ}\text{C}$  from 1500 onward and about  $0.25^{\circ}\text{C}$  after 1800.

Running correlations between annual Alpine, winter (DJF) and summer (JJA) temperatures are significantly positive for the whole reconstruction period and confirm the overall temporal stability of the reconstruction (not shown).

#### 3.2. Alpine precipitation variability 1500–2003

Figure 3 presents the average Alpine annual, winter (DJF) and summer (JJA) precipitation sum anomalies (mm) with regard to the 1901–2000 mean from 1500 to 2003 and the corresponding extremes prior to 1900 (numbers). Annual Alpine precipitation sums before 1800 were low, the 1840s very wet. Dry periods prevailed around 1860 and after 1945. In the annual precipitation time series, fast transitions from wet to dry conditions around 1830, 1920 and 1945 are recorded. The year 1540 was the absolute driest of the last 500 years (anomaly of  $-360$  mm compared with the annual precipitation sum of around 1200 mm for the twentieth century) and 1627 the absolute wettest (anomaly of  $+305$  mm). Table II presents all positive or negative precipitation extremes for the annual, winter, and summer time series. The uncertainties of the reconstruction are  $\sim 90$  mm for the reconstruction from 1500 onward and decrease to 60 mm for the 1700–1850 period and to 35 mm after 1850.

Figure 3(b) shows winter precipitation anomalies between 1500 and 2004. Dry winters occurred in the second half of the nineteenth century, and some very dry winters between 1990 and 1994. Wet winter conditions are seen in the 1670s, 1720s, 1910s and the years 1950 to 1990. It is remarkable that positive

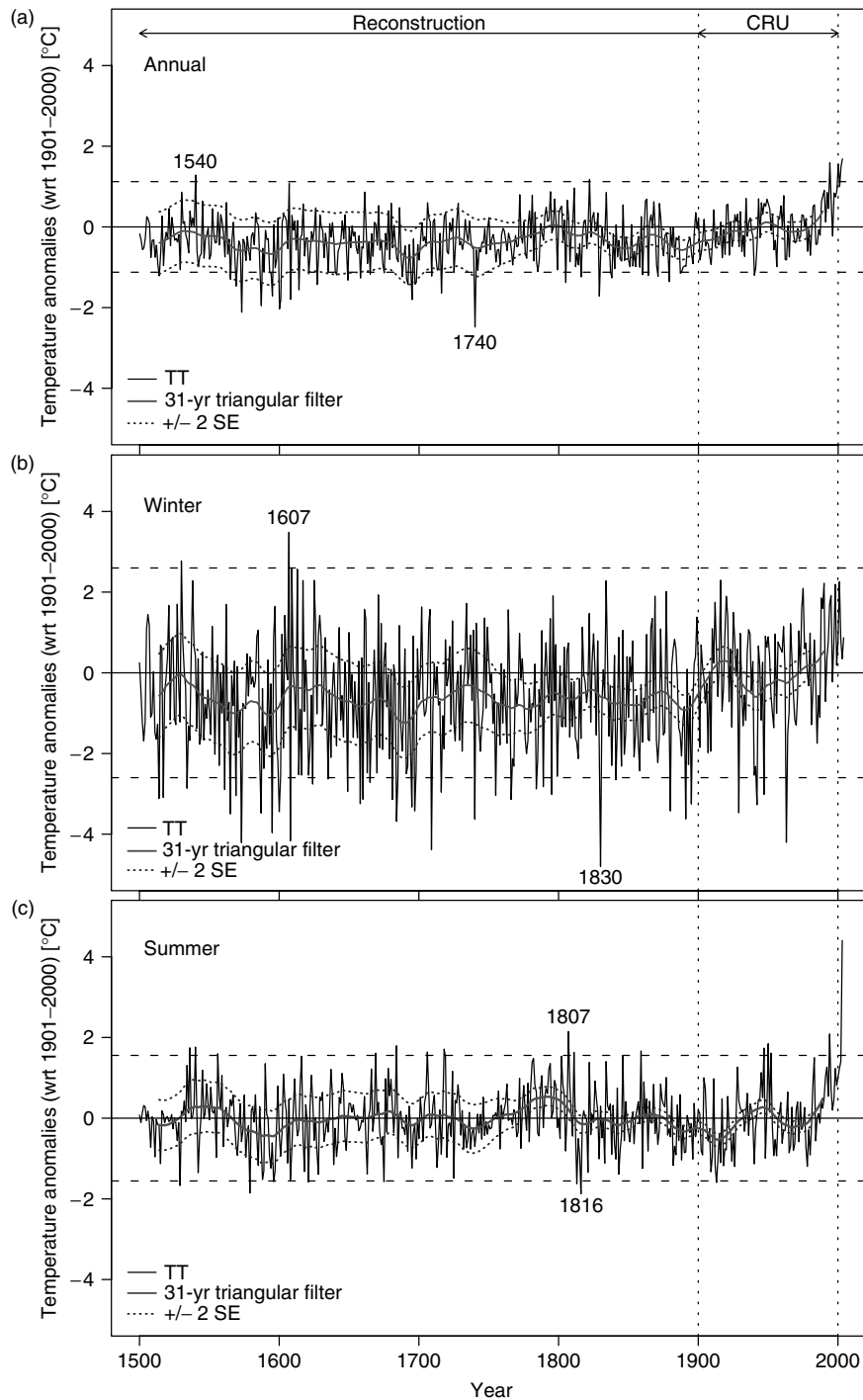


Figure 2. (a) Annual (January–December) mean Alpine temperature anomalies (reference period 1901–2000) from 1500 to 2003 (black lines, denoted as TT). The anomalies for the period 1500 to 1900 are the reconstructions; the values from the twentieth century are derived from the Mitchell *et al.* (2004) data-set. The data from 2001 to 2004 stem from GISS NASA surface temperature analysis (updated from Hansen *et al.* (1999, 2001); given on a  $1^\circ \times 1^\circ$  resolution; <http://www.giss.nasa.gov/data/update/gistemp/>). The thick line is the 31-point triangular low pass filtered time series. The dotted horizontal lines indicate the  $\pm 2$  standard deviations of the twentieth century. The uncertainties are given by the  $\pm 2$  standard errors (SE). (b) and (c): same as (a), but for mean winter (DJF, 1500–2004) and summer (JJA) temperature anomalies, respectively. Numbers indicate the absolute extremes

Table I. Annual, winter (DJF), and summer (JJA) temperature extremes exceeding the  $\pm 2$  standard deviations of the twentieth century mean. TT+ (TT-) stands for positive (negative) extremes

Annual TT+	Annual TT-	Winter TT+	Winter TT-	Summer TT+	Summer TT-
1540	1514	1530	1514	1536	1529
1822	1565	1607	1517	1540	1579
1994	1569	1609	1534	1556	1596
2000	1573		1561	1669	1621
2002	1587		1565	1684	1675
2003	1593		1569	1706	1813
	1594		1573	1718	1816
	1595		1587	1807	1913
	1600		1595	1811	
	1601		1600	1859	
	1608		1608	1947	
	1614		1624	1950	
	1621		1635	1952	
	1627		1649	1994	
	1641		1658	2003	
	1649		1660		
	1658		1665		
	1665		1681		
	1675		1684		
	1688		1695		
	1691		1697		
	1692		1709		
	1695		1716		
	1697		1740		
	1698		1755		
	1709		1766		
	1716		1784		
	1725		1789		
	1740		1795		
	1805		1830		
	1816		1841		
	1829		1880		
	1838		1891		
	1860		1895		
	1864		1929		
	1871		1942		
	1879		1947		
	1887		1963		
	1940				

winter extremes exceeding two standard deviations are observed only in the twentieth century. 1915 was the wettest Alpine winter (anomaly of +141 mm with regard to the twentieth century winter mean of 245 mm), and 1858 the driest winter (-132 mm). Uncertainties are high prior to 1770 (190 mm). From 1770 onward, they decrease to values around 90 mm.

Interannual summer precipitation (Figure 3(c)) shows three prominent dry periods: around the 1540s, after 1770, and after 1860. Also, after 1970 a decrease in summer precipitation is found. Very wet summers occurred from 1550 to 1700. 1540 was the absolute driest summer since 1500 in the Alps (anomaly of -164 mm with regard to the twentieth century mean summer precipitation sums of 352 mm), and the summer of 2003 was of comparable magnitude. 1663 was the absolute wettest summer (+148 mm). The uncertainties for the summer

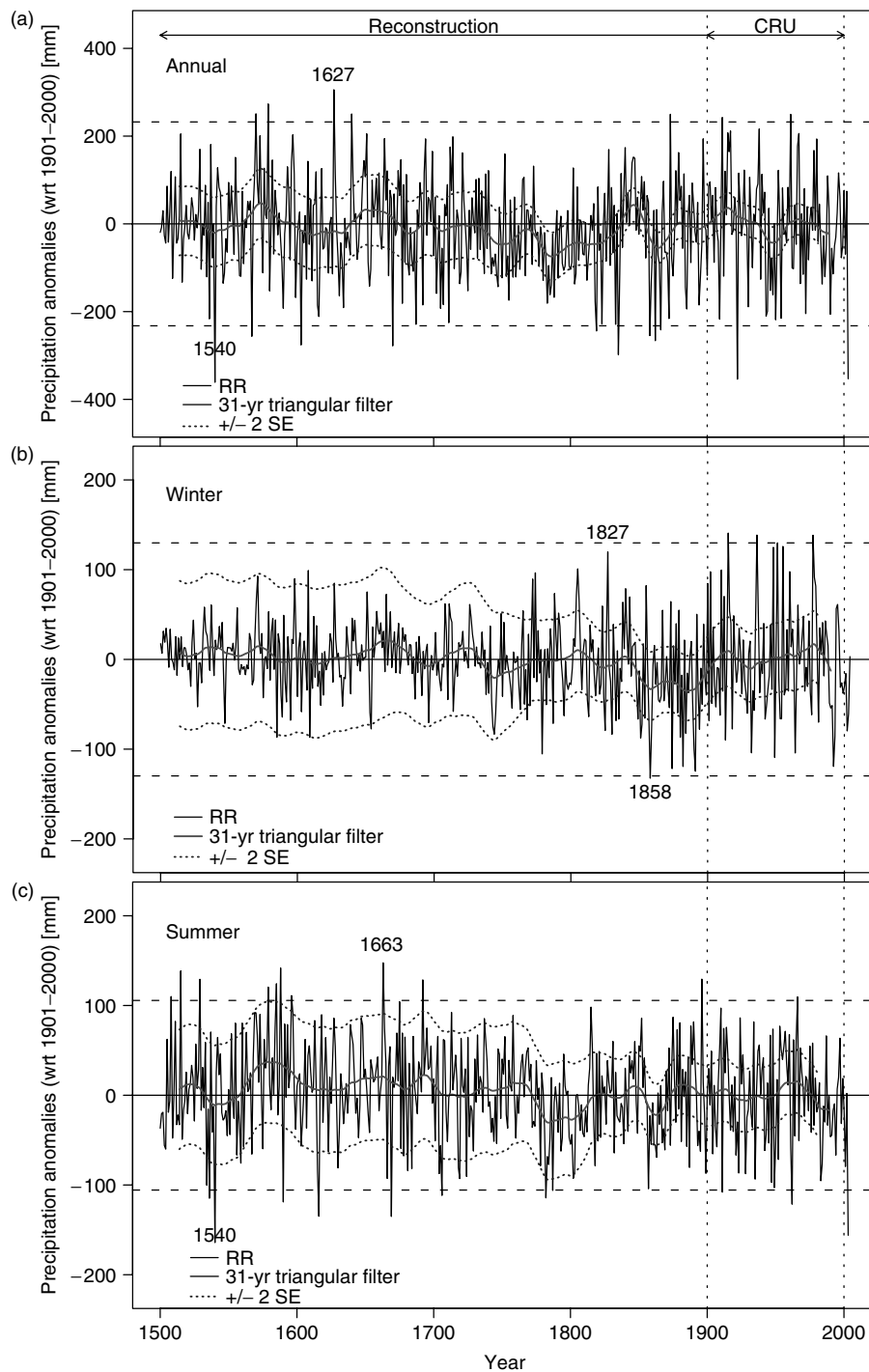


Figure 3. (a) Annual (January–December) mean Alpine precipitation anomalies (reference period 1901–2000) from 1500 to 2003 (black lines, denoted as RR). The anomalies for the period 1500–1900 are the reconstructions; the values from the twentieth century are derived from the Mitchell *et al.* (2004) data-set. The data from 2001 to 2004 stem from CMAP analysis of precipitation (updated from Xie and Arkin (1997); given on a  $2.5^\circ \times 2.5^\circ$  resolution; [http://www.cpc.ncep.noaa.gov/products/global\\_precip/html/wpage.cmap.html](http://www.cpc.ncep.noaa.gov/products/global_precip/html/wpage.cmap.html)). The thick line is the 31-point triangular low pass filtered time series. The horizontal dotted lines indicate the  $\pm 2$  standard deviations of the twentieth century. The uncertainties are given by the  $\pm 2$  standard errors (SE). (b) and (c): same as (a), but for mean winter (DJF, 1500–2004) and summer (JJA) precipitation anomalies, respectively. Numbers indicate the absolute extremes

Table II. Annual, winter (DJF), and summer (JJA) precipitation extremes exceeding the  $\pm 2$  standard deviations of the twentieth century mean. RR+ (RR-) stands for positive (negative) extremes

Annual RR+	Annual RR-	Winter RR+	Winter RR-	Summer RR+	Summer RR-
1570	1540	1827	1858	1508	1536
1579	1567	1915	1874	1515	1540
1627	1603	1936	1882	1529	1590
1640	1669	1948	1891	1579	1616
1872	1818	1951	1992	1585	1669
1910	1834	1955		1588	1706
1960	1857	1977		1596	1782
	1861			1663	1787
	1865			1692	1911
	1921			1896	1962
	2003			1966	2003

reconstruction are lower than for winters. They range from 145 mm for the 1500–1770 period to 80 after 1800.

Regarding the temporal stability of the reconstruction, the annual Alpine precipitation shows positive correlations with winter (DJF) and summer (JJA) precipitation prior to 1659. Afterwards, running correlations are non-significant (not shown). It seems that during periods when seasonal precipitation reconstructions are performed (1500–1659), the temporal stability and seasonality of the reconstruction are not fully certain.

### 3.3. Winter and summer extremes 1500–1900

Figures 4(a) and (c) show the spatial representations of the coldest Alpine winter and warmest summer during the reconstruction period (1500–1900), Figures 4(e) and (g) exhibit the wettest winter and driest summer, and Figures 4(b), (d), (f), and (h) show the corresponding averaged sea level pressure (SLP) fields from Luterbacher *et al.* (2000, 2002a).

The absolute coldest winter in the Alpine area occurred in 1829/30 (Figure 4(a)). The largest anomalies, up to  $-7^{\circ}\text{C}$ , are found in northeastern Austria. The southern part of the French Alps shows anomalies up to  $-3^{\circ}\text{C}$ . The dotted lines reveal the distribution of RE, indicating that the reconstructions are most reliable in the central part of the Alps. However, no skilful reconstruction is made for a part of the French Alps, where RE values are around zero.

Note that the SLP reconstruction of Luterbacher *et al.* (2000, 2002a) is not fully independent of the reconstructions presented here. The pressure field for the cold winter 1829/30 (Figure 4(b)) indicates a strong blocking of the westerlies connected with a cold temperature pattern. A cold anticyclone with strong northeasterly airflow prevailed over northeastern Europe, connected with advection of cold air masses to Central Europe. The SLP anomalies (dotted lines, 1901–2000 reference period) indicate that the pressure tendency over the Alps was similar to twentieth-century conditions. The highest positive pressure anomalies (more than 10 hPa) are found over Scandinavia.

The warmest Alpine summer (1807; Figure 4(c)) in the reconstruction period shows anomalies east of  $10^{\circ}\text{E}$  with maximum departures of  $+2.6^{\circ}\text{C}$ . The southwestern part of the Alpine region exhibits smaller anomalies. The reconstructions are skilful over the whole Alpine region except for the French Alps, as expressed by generally high RE values. The SLP field for the hot summer 1807 (Figure 4(d)) was dominated by a strong Azores High (AH) stretching towards Central Europe. The anomalies over the Alps were 2 hPa higher than the twentieth-century mean, which is interpreted by a strong influence of the AH.

Although 1915 was the wettest winter for the Alpine region, here we focus on the anomalous wet winter of 1826/27 (Figure 4(e)), which was the wettest in the reconstruction period. Wet conditions prevailed over Slovenia with anomalies up to  $+350$  mm. The whole Alpine region was wet except the western part of Switzerland and the neighbouring France. However, for those regions with the strongest anomalies, the

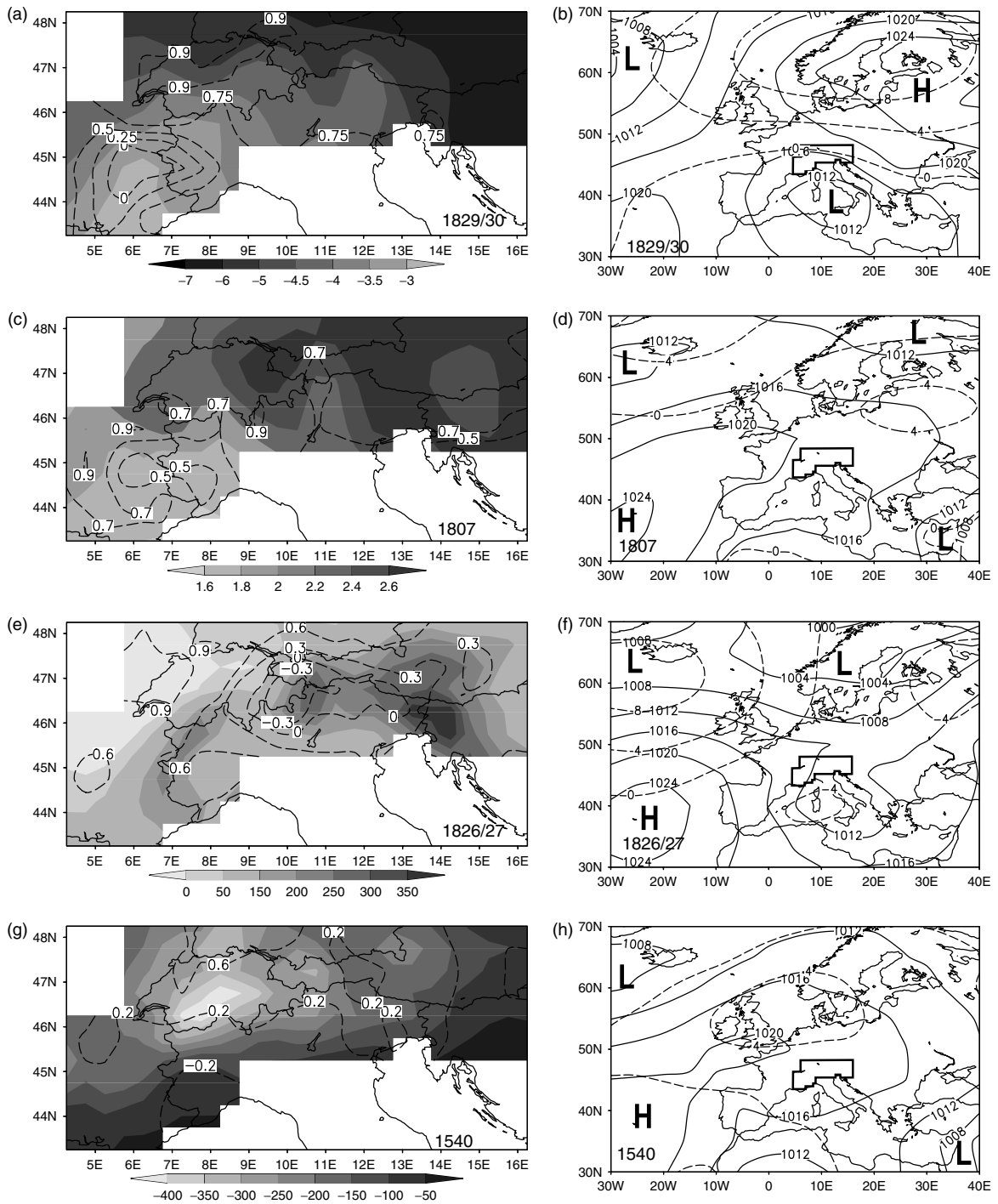


Figure 4. Seasonal anomaly temperature and precipitation patterns of the extremes (extremes minus long-term mean of 1901–2000) derived from figures 2 and 3 (see numbers). (a) Temperature anomaly pattern for the coldest winter 1829/30 of the reconstructed period. The dotted lines exhibit the model performance (RE) pattern for the anomalous cold winter 1829/30. For areas with RE > 0, a meaningful reconstruction can be expected. (c) same as in (a), but for the warmest summer, 1807. (e): same as in (a) and (c), but for precipitation anomalies for the wettest winter, 1826/27, within the reconstructed period. (g) same as in (c) but for the driest summer, 1540. (b), (d), (f), and (h): The corresponding SLP pressure fields for the extremes. The solid lines exhibit the averaged SLP values; the dotted lines reveal the SLP anomalies (reference period 1901–2000). The black box marks the Alps

reconstruction quality is low and even negative RE values are observed over the central Alps. The pressure field for the wet winter 1826/27 (Figures 4(f)) is characterized by a strong negative anomaly west of the British Isles. South of the Alpine region, average pressure conditions are lower than in the twentieth century (up to 4 hPa), suggesting that many low-pressure systems from the Mediterranean approached the Alps.

The extremely dry summer of 1540 is presented in Figure 4(g). The studied region was divided in two parts, a very dry northern and a less dry southern area with a very dry centre situated over the Swiss Alps. RE values are skilful in the North and modest for the South. The SLP field for the dry summer of 1540 (Figure 4(h)) shows similarities to the warmest reconstructed summer of 1807. An extension of the AH reached Central Europe, and northern Europe was dominated by higher than twentieth century pressure conditions. This might indicate a break in moisture transport from the ocean to the continent. Anomalies over the Alps were 2 hPa higher than the 1901 to 2000 average.

### 3.4. Influence of the NAO on the Alps since 1659

Central Europe and the Alps are situated in a band of low correlations of the influence of the NAO on temperature or precipitation patterns. This forcing enhances with greater distance north or south of the Alpine area (Hurrell and van Loon, 1997). At lower elevations the NAO signal may be weak or even absent whereas higher elevation sites in the Alps are sensitive to the NAO influence (Beniston *et al.*, 1994; Beniston and Jungo, 2002). Beniston and Jungo (2002) found that the positive phase of the NAO (enhanced westerlies over western Europe) leads to anomalously low precipitation and higher than average temperatures, particularly from late autumn to early spring, in southern and Central Europe (including the Alps and the Carpathians) during the twentieth century. Thus, we focus on the influence of the NAO on Alpine temperature and precipitation variability during winter.

Thirty-one-year running correlations between the extended winter (DJFM) North Atlantic Oscillation Index (NAOI; Cook *et al.*, 2002) and the Alpine extended winter (DJFM) temperature and precipitation time series from 1659 to 2000 were computed (Figure 5). Prior to 1659, only seasonal (DJF) Alpine reconstructions are available.

Winter temperatures show positive correlations with the NAOI. These correlations are neither stable over time nor always significant on a 95% confidence level determined using a Monte Carlo approach. From 1690 to 1750 (+/–15 years, due to the 31-year window), and between 1850 and 1880 Alpine temperatures are uncorrelated with the NAOI. Overall, temperatures show four significant positive correlated periods. A first

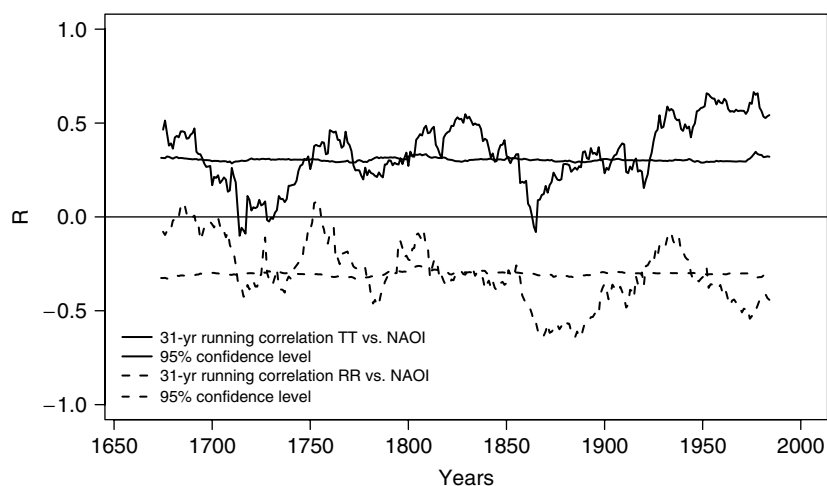


Figure 5. 31-year running correlation between the winter (DJFM) NAOI reconstruction by Cook *et al.* (2002) and Alpine winter (DJFM) temperatures (thick solid line), and the Alpine winter precipitation (thick dotted line) from 1659 to 2000. The thin solid black line represents the 95% significant levels determined using a Monte Carlo simulation for temperature, the thin dashed line those for precipitation. TT stands for temperature, RR for precipitation

short period appears from 1675 to 1690, followed by 1750 to 1770, and then 1800 to 1850. Finally, the fourth and strongest positively correlated phase is detected for the filtered years 1920 to 1965. During these periods, positive (negative) NAO conditions caused mild (cold) Alpine temperatures.

The Alpine winter precipitation shows negative correlations with the NAOI. Again, these relations are not stable over time and not always significant. From 1675 to 1700, and around 1750, the Alpine winter precipitation is not correlated with the NAOI. Significant periods are detected from 1710 to 1740 (with a break around 1730), 1780 to 1790 and after 1860, with a distinct relapse from 1920 to 1940, that exceed the 95% confidence level. During these periods, a high (low) NAOI value caused dry (wet) Alpine climate conditions.

#### 4. DISCUSSION

A comparison of smoothed regional (Luterbacher *et al.*, 2004) and large-scale temperature reconstructions (Jones *et al.*, 1998) and homogenized instrumental data from the Alps (Böhm *et al.*, 2001) with the new reconstruction presented here reveals similarity in the lower frequency domain (Figure 6(a)). The global and Northern Hemispheric warming at the end of the twentieth century (e.g. IPCC, 2001; Folland *et al.*, 2001) and in Europe (e.g. Luterbacher *et al.*, 2004) is also prominent in the greater Alpine region. It occurred in mainly two stages: between 1880 and 1945 and since 1975. A period of warmth around 1800 and periods of distinct cooling roughly around 1600, 1700 and 1900 are seen in all records. Pfister (1992, 1999) and Luterbacher *et al.* (2004) found similar cooling periods for Europe. A cooling between 1725 and 1750 appears in the Alpine reconstruction, whereas the European reconstruction shows a warming trend. From 1850 to 1880, a period of warmth is found in both Alpine reconstructions, unlike the European temperatures. Alpine temperature reconstructions seem to reproduce a distinct regional signal for these two periods.

Of special interest is the difference in amplitude between the CRU data used in this study and the Böhm *et al.* (2001) Alpine temperature record during the 1901–2000 reanalysis period, although both time series are highly correlated and almost fully dependent. The latter record is an interpolation on a  $1^\circ \times 1^\circ$  grid over the greater Alpine region by using 105 low-elevation (<1500 m a.s.l.) and 16 high-elevation (>1500 m a.s.l.) of quality-checked and homogenized temperature stations within this region. The greatest part of the systematic difference is an expression of the very strict homogenization procedure and outlier detection applied to the station data used for the Böhm *et al.* (2001) record. The intensive use of station history information in this study also provided an explanation for the addressed amplitude increase. In the twentieth century, there was a systematic trend to relocate specifically the traditional long-term measuring sites from the historic centres of cities to airport sites in rural surroundings. This suggested respective negative adjustments of the older (more urban) *versus* the modern (more rural) sites and thus confirmed the pure mathematical results of relative homogeneity testing. There may still be existing limitations of an older version of the CRU data on a  $5^\circ \times 5^\circ$  grid (Jones *et al.*, 1999), developed for the investigation of large-scale temperatures, in describing regional climate variability in the complex terrain of the Alpine region, but to our knowledge no limitation is reported of the newest version of the CRU data (Mitchell *et al.*, 2004) in describing Alpine climate. An interesting feature visible in our reconstruction as well as in the Böhm *et al.* (2001) record is the distinct temperature peak near 1800. Instrumental evidence tells that it is mainly caused by spring and summer and nearly vanishes in autumn and winter. It seems to be a typical Central European feature also present in some physical proxies in the region. For larger regions (Europe, the Northern Hemisphere), it is less distinct. As there is also some contradicting evidence from other proxies, it should be studied more intensively and more sophisticatedly (multi-proxy plus documentary plus instrumental plus physical forcings) in the future.

Over the past 500 years, the Jones *et al.* (1998) warm season reconstruction correlates well with annual Alpine temperatures; however, they are not fully independent. Frank and Esper (2005) present comparisons between Alpine tree-ring based temperature reconstructions and instrumental data. They found that the response of ring-width data is not strictly limited to summer season temperatures, but also carries an annual signal particularly in the lower frequency domain (e.g. after decadal smoothing). Esper *et al.* (2002) and Cook *et al.* (2002) found significant correlations between land-only annual and warm season temperatures for the

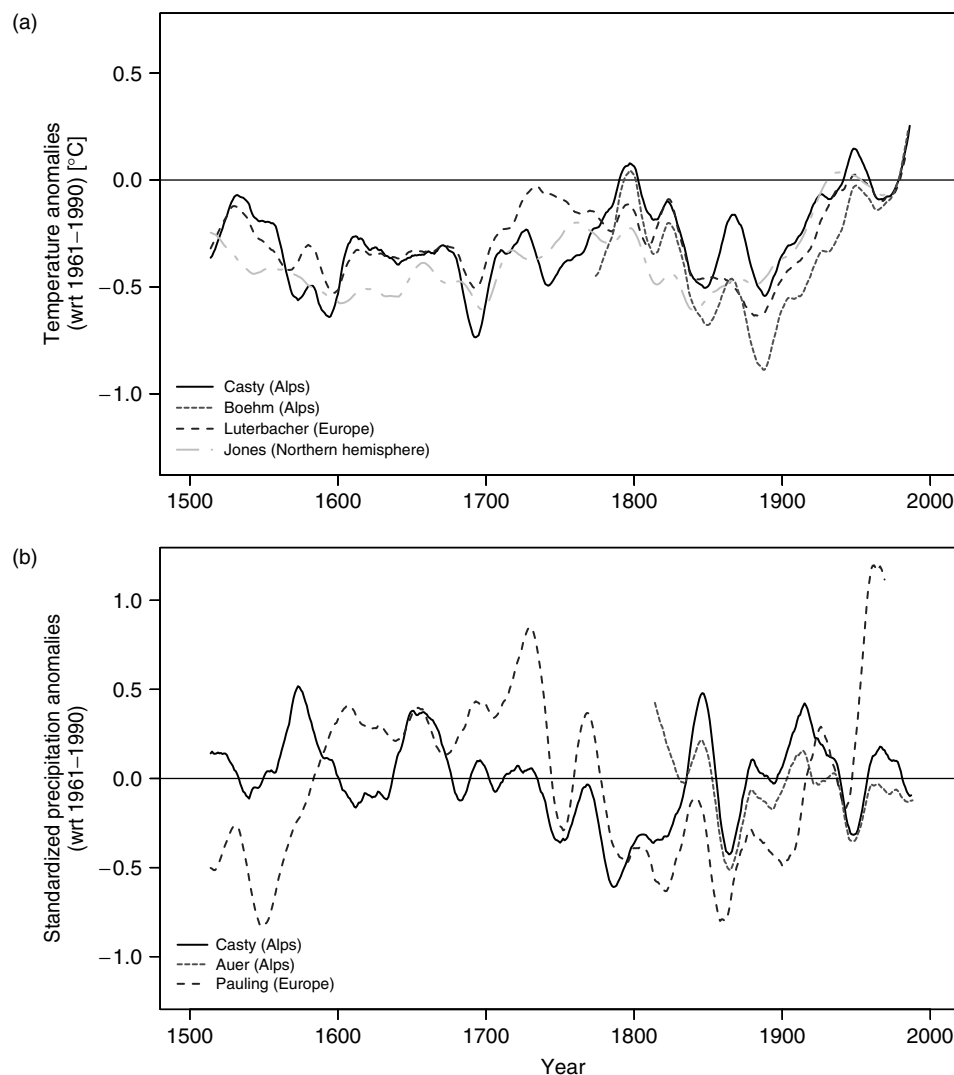


Figure 6. (a) Smoothed (31-year triangular filter) time series of temperature reconstructions for the Northern Hemisphere (dashed-dotted line: Jones *et al.* 1998; 1500–1991), Europe (dashed line: Luterbacher *et al.* 2004; 1500–2000), and the Alpine region (dotted line: Böhm *et al.*, 2001; 1760–1998; solid line: this study, 1500–2000). The temperature anomalies are calculated with regard to the 1961–1990 mean. Note that for comparison reasons the Böhm *et al.* (2001) grid is matched with the same region as used in this study. Jones *et al.* 1998 is published as summer temperature reconstruction. (b): same as (a) but for standardized annual precipitation anomalies (reference period 1961–1990) for Europe (dashed line: 30°–67°N and 10°W–40°E; Pauling *et al.*, 2005; 1500–1983) and the Alpine region (dotted line: Auer *et al.*, 2005; 1800–2002; solid line: this study; 1500–2000). The grid points of Auer *et al.* (2005) are interpolated to values of relative anomalies denoted as percentages of the station mean 1961–1990 for the corresponding grid point and not in absolute precipitation amounts in mm. Therefore, all precipitation anomalies are standardized. For comparison reasons, the Auer *et al.* (2005) grid is matched with the same region as used in this study

extratropics in the Northern Hemisphere for the period 1856–2000 after they applied decadal smoothing. This effect seems to be detectable in case of the Jones *et al.* (1998) data also.

Regional temperature changes have generally larger amplitudes of variations than those averaged over large areas (e.g. Mann *et al.*, 2000; Luterbacher *et al.*, 2004; Jones and Mann, 2004; Brázdil *et al.*, 2005; Xoplaki *et al.*, 2005). This is not clearly found for the reconstruction presented in this study. Although it shows higher temperature variations than for the Northern Hemisphere, the differences in the amplitude are small in comparison with the European temperatures.

The years 1994, 2000, 2002 and particularly 2003 were the warmest since 1500 in the greater Alpine region, with 2003 being  $+1.7^{\circ}\text{C}$  warmer than the mean of the twentieth century. It was characterized by an extremely warm spring and a persistent heatwave during summer (Luterbacher *et al.*, 2004; Schär *et al.*, 2004; see also Figure 2(c)). Interestingly, extremely warm spring and warm summer temperatures also characterized the warmest year prior to 1900, 1540. Glaser *et al.* (1999) and Jacobeit *et al.* (1999) report extremely dry conditions and persistent high-pressure conditions stretching from Central Europe to Poland from March to August, although there is no independent evidence. The absolute coldest year for the last 500 years in the Alpine region was 1740. Pfister (1999) describes very cold conditions from October 1739 to May 1740. Low-elevation lakes in the Swiss Alpine foreland were completely frozen. Wanner and Luterbacher (2002) reconstructed the winter 1739/1740 and addressed a strong blocking pattern with extremely cold conditions over Central Europe. Especially the spring of 1740 was extremely harsh in Central Europe (Glaser, 2001).

Figure 6(b) comprises the smoothed European annual precipitation reconstruction of Pauling *et al.* (2005), the regional Alpine reconstructions by Auer *et al.* (2005) and the data used in this study. The Auer *et al.* (2005) gridded reconstruction ( $1^{\circ} \times 1^{\circ}$ ) starts in 1800 and is derived from 192 homogenized precipitation station series all over the Alpine region. The Pauling *et al.* (2005) precipitation reconstruction, plotted from 1500 onward, is based on the same predictands (Mitchell *et al.*, 2004) and methodology as described in this study and includes a large number of proxy data and early instrumental precipitation time series from Europe. European and Alpine precipitation sums are not comparable, and therefore all three reconstructions are standardized to anomalies with regard to the 1961–1990 mean. The individual uncertainties of each reconstruction are not considered. Note that both the Auer *et al.* (2005) and the Pauling *et al.* (2005) data are not independent of the Alpine precipitation reconstruction presented in this study. The often-cited positive feedback mechanism between increasing temperatures and increasing precipitation due to an enhanced water cycle for the last three decades (IPCC, 2001) is not detectable in the averaged Alpine series. The European precipitation reconstruction shows a significant increase of precipitation in the late twentieth century. Schmidli *et al.* (2002) found positive linear trends for precipitation during winter for the northwestern part of the Alps but negative ones for autumn in the southeast of the Alps for the 1901–1990 period. All three reconstructions show an increase in the precipitation after 1930, especially the time series for Europe. After a dry phase around 1800, the 1840s were wet in the Alpine region and maybe responsible for the last advance of the Alpine glaciers around 1850–1860. The three reconstructions correlate well; however, after 1800 the Alpine record of Auer *et al.* (2005) shows a decrease in precipitation amount unlike the other two reconstructions. This is basically due to the homogenization procedure applied to the precipitation series. Early precipitation series were systematically installed much higher above ground than today. Auer *et al.* (2005) consequently increased the early precipitation series by up to 10%. However, trends on the sub-regional scale could also lead to the differences. We consider the Alps as a region that comprises a variety of well-known climatic differences in different subregions and seasons (e.g. Wanner *et al.*, 1997). The quality of the CRU data (Mitchell *et al.*, 2004), used as a predictand in this study to capture sub-regional effects in precipitation distribution, such as the enhancement of precipitation along the Alpine foothills or the shielding of inner-Alpine valleys (Frei and Schär, 1998), remains unknown. The period from 1600 to 1720 was wet in the European reconstruction. The Alpine time series also shows a peak around 1650. The very wet period around 1720 for Europe is not found for the Alps. Between 1590 and 1630, the two time series proceed in the opposite direction. This may be an indication of separated precipitation regimes for Europe and the Alps.

Beside 1921 and 2003, 1540 was the driest year in the Alpine region for the last 500 years (Figure 3(a)). These years were characterized by strong negative precipitation anomalies during the warm season (Figure 3(c)). Pfister (1999) reported extreme drought conditions (probably the most persistent drought for the last 700 years) for Switzerland during the summer of 1540, and Glaser *et al.* (1999) and Glaser (2001) reported the same for Central Europe. The wettest year, 1627, was characterized by extreme wet and cold conditions from winter until the beginning of July for Central Europe (Pfister, 1999; Glaser, 2001), denoted by e.g. a delay of the cherry-tree blooming of three weeks, floods, snowfall in June and a poor vintage in autumn.

The most prominent source of climate variability in the North Atlantic/European region is the NAO. Its influence is strongest in wintertime (e.g. Wanner *et al.*, 2001; Hurrell *et al.*, 2003), and the reaction of Alpine weather and climate to this phenomenon is complex (Wanner *et al.*, 1997; Beniston and Junco, 2002). During

the twentieth century, Beniston and Jungo (2002) found anomalously low precipitation amounts and higher than average temperatures for the Alps during positive NAO phases, especially during winter. The opposite climate behaviour is found for negative NAO states. The Alpine winter (DJFM) temperatures from 1659 to 2000 are positively correlated with the independent NAOI of Cook *et al.* (2002). Winter precipitation is negatively correlated (Figure 5) and supports the findings of Beniston and Jungo (2002). These correlations, however, are not stable over time and not always significant. It is stated that this is firstly caused by the orientation of the Alps in a band of generally low correlations with the NAO (Hurrell and van Loon, 1997; Wanner *et al.*, 1997). Beniston *et al.* (1994) and Beniston and Jungo (2002) state that high-elevation sites are more sensitive to changes in NAO. Therefore, secondly, the utilization of mainly low-elevation stations for our reconstruction and the complex topography of the Alps possibly lead to lowered correlations. Thirdly, it could be traced back to the possible involvement of other atmospheric processes during uncorrelated periods. It is still debated if other circulation modes dominated during such periods (Luterbacher *et al.*, 1999; Slonosky *et al.*, 2001; Casty *et al.*, 2005a). Jacobeit *et al.* (2003) demonstrated which circulation modes dominated since the mid-seventeenth century over the North Atlantic–European region. The interpretation of these correlations should be made with caution owing to the limited quality of the reconstruction and the choice of the considered regions (Schmutz *et al.*, 2000; Luterbacher *et al.*, 2002a,b and 2004; Cook *et al.*, 2002). Figure 7 simplifies the dynamical influence of the NAO on the Alpine temperature and precipitation during winter for periods with significant correlations. It attempts to represent the connection between the northeast Atlantic sea surface temperatures (SSTs) and the two most important pressure centres, the Icelandic Low (IL) and the AH, with the intensity of the polar jet and the related catchment area of the storm tracks. It also shows the resulting pressure field tendencies over the Alpine region. We assume the atmosphere is equivalent-barotropic on climatological timescales (Palmer and Sun, 1985; Wanner *et al.*, 2001) and very strong SST anomalies modify the atmospheric pressure field with a certain time lag of months (Czaja and Frankignoul, 1999). The formation of such anomalies is not in the focus of this study. In the case of a positive NAO phase (Figure 7(a)), SST anomalies are strongly negative south of Greenland and positive around the Azores. The two pressure centres of action (IL and AH), which are normally situated slightly downstream of the SST anomalies, are intensified and a strong polar front jet appears. The jet-axis then points from southwest to northeast. The Alps are located southeast of the exit zone of the jet and therefore southeast of the main storm tracks, in the divergence zone of the jet. In this area, the ageostrophic displacement of atmospheric mass leads to an increased atmospheric pressure tendency over the Alps. This concept is also known as the Ryd–Scherhag divergence theory (Scherhag, 1948). The increased pressure tendency over the Alps results in relatively high temperatures at higher-elevated sites and generally lowered precipitation amounts. In the opposite case (negative phase of the NAO, Figure 7(b)), the North Atlantic shows positive SST anomalies in its northern area near Greenland and negative ones around the Azores. Therefore, the two pressure centres are not fully developed; the north to south pressure gradient is rather weak. The polar jet is shifted to the south and weakened compared with the positive NAO phase. Negative pressure anomalies can be observed during such periods especially south of the Alps. This is in agreement with Wanner *et al.* (1997) and Beniston and Jungo (2002). During summer, the atmospheric circulation over the studied area is often dominated by weak pressure gradients. Therefore, regional effects, e.g. thermally driven wind systems or thermally induced storm activities, influence the weather conditions. The main pressure centres of action, namely, the IL and the AH, shift toward the west during this season (Wanner *et al.*, 1997; Davis *et al.*, 1997; Portis *et al.*, 2001).

## 5. CONCLUSIONS

We studied the annual and seasonal variability of reconstructed temperature and precipitation over the European Alpine region ( $\sim 43.25^{\circ}$ – $48.25^{\circ}$ N and  $4.25^{\circ}$ – $16.25^{\circ}$ E) since 1500. The years 1994, 2000, 2002 and 2003 were the warmest since 1500. Three prominent cooling periods occurred around 1600, 1700 and 1900. The transition from cold conditions prior to 1900 to present day warmth is found in annual, winter, and summer Alpine temperatures. These periods are also seen in reconstructions of the Northern Hemisphere and Europe. The reconstructions used for the comparison are dependent on the presented data, i.e. they share common

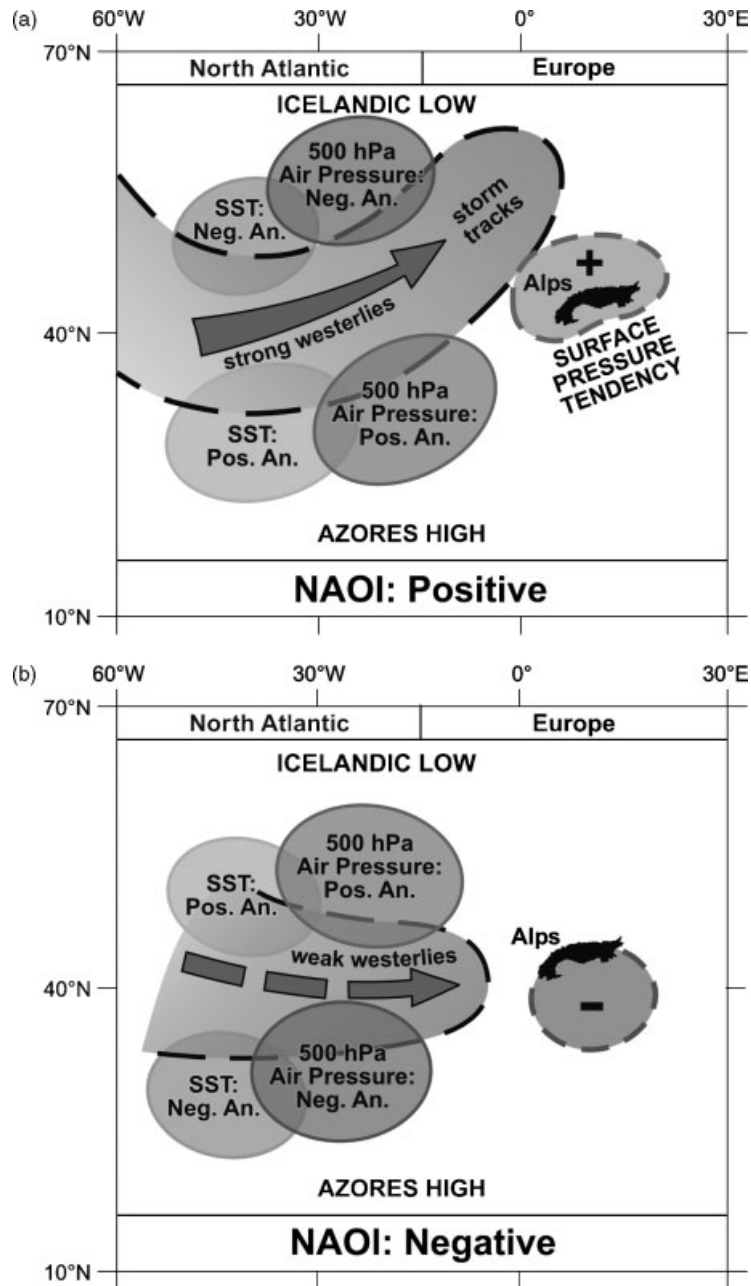


Figure 7. A schematic illustration of the sea surface temperature anomalies, the main pressure centres of action (Icelandic Low and the Azores High), the location of the polar jet and the direction of the storm tracks for the two phases of the NAO affecting the pressure tendency of the Alps during winter. (a) reveals the positive phase of the NAO, (b) the negative phase of the NAO

predictors. Very cold winters occurred at the turn of the eighteenth century, and warm winters prevailed in the early sixteenth and seventeenth century as well as in the 1920s and 1970 onwards. Warm summers were experienced around 1550, during the seventeenth century and the second half of the eighteenth century and from 1970 onward. The uncertainties of the reconstruction are generally low for annual and summer Alpine temperature with values of around 0.7 °C between 1500 and 1800 and 0.2 °C from the nineteenth century to the present. The uncertainties for winters are roughly 1.1 °C for the 1500–1800 period and 0.6 °C thereafter.

The Alpine precipitation time series do not indicate significant trends. The expected increase in precipitation as a result of increased temperatures for the warm period at the end of the twentieth century (IPCC, 2001) is not revealed for the Alps. 1540 was the driest year over the last 500 years. Comparison of precipitation reconstructions for Europe and the Alps reveal good correspondence with the Alpine reconstruction presented in this study; however, these reconstructions are not entirely independent. The uncertainties of the reconstruction were high prior to 1770, especially for winters (190 mm) and summers (145 mm). This is due to decreasing numbers of predictors. Annual Alpine precipitation showed lower uncertainties during that period (90 mm).

As far as the extreme events are concerned, the question is still open whether monthly resolution data properly capture such features. Independent SST and air pressure reconstructions are needed to study the processes modulating extreme events at different space and time scales.

Running correlations between the NAOI and temperature/precipitation patterns in the European Alpine region are only significant during certain periods of the extended winters (DJFM) between 1659 and 2000. The NAOI shows mainly positive correlations with temperatures and negative values for precipitation. These correlations, however, are temporally unstable. This suggests that the Alps are situated in a band of rather weak and varying forcing of the NAO and other atmospheric circulation modes may dominate during low correlation periods.

The validation and calibration of the presented reconstruction is based on the Mitchell *et al.* (2004) data. By extending gridded data-sets of higher spatial and temporal resolution for the Alps (e.g. Frei and Schär, 1998; Auer *et al.*, 2000, 2001b, 2005; Böhm *et al.*, 2001; Schmidli *et al.*, 2001; Gyalistras, 2003; Kettle and Thompson, 2004) back in time we may improve the reconstruction of climatic parameters for the European Alps to better assess climate change on regional scales. In particular, another assessment for precipitation on a sub-regional scale over the Alps seems to be worthwhile.

The presented reconstructions are useful for the validation of proxy-based reconstructions for the Alpine region or the evaluation of regional past climate model runs. Temperature and precipitation grids are reconstructed independently (Wanner and Luterbacher, 2002; Casty *et al.*, 2005b). Therefore, dynamical processes involving both variables can be studied and related.

#### ACKNOWLEDGEMENTS

We thank the Swiss National Science Foundation for supporting this study through its National Center of Competence in Research (NCCR) in Climate. We also thank Dr I. Auer and Dr W. Schöner for kindly providing the data of the projects CLIVALP (Austria FWF, P1576-N06), CLIMAGRI (the Italian CNR Special Project 02-03/05/97-037681) and ALP-IMP (EU, EVK2-CT-2002-00148). Dr T. Mitchell kindly provided the gridded temperature and precipitation data (CRU TS 2.0). The Northern Hemisphere temperature reconstruction is available through the NOAA Paleoclimatology World data center (WDC) link: <http://www.ngdc.noaa.gov/paleo/>. Dr R. Rickli and Dr M. Grosjean are acknowledged for fruitful discussions on the manuscript.

APPENDIX 1. The collection of all climatological time series (predictors, in chronological order) used for the temperature reconstruction. Denoted are the station elevation (H) in meters, the latitudes (Lat) in degrees north, the longitude (Lon) in degrees east, the start year of the time series, the station name and finally the country. Note that the historical indices derived from documentary evidence are marked with (I) in the station name column

H (m)	Lat (N+)	Lon (E+)	Start year	Station name	Country
130	47.5	19	1500	Ancient Hungary (I)	Hungary
469	50	14.4	1500	Czech Republic (I)	Czech Republic
565	~46.5	~7.35	1500	Mittelland (I)	Switzerland
~10	B, Lux, NL		1500	Low countries (I)	B, Lux, NL

(continued overleaf)

APPENDIX 1. (*Continued*)

H (m)	Lat (N+)	Lon (E+)	Start year	Station name	Country
~300	~48	~11.4	1500	Southern Germany (I)	Germany
0	D, DK coasts		1501	Baltic sea-ice (I)	D, DK
2	52.1	5.18	1634	De Bilt (I)	Netherlands
~100	51.47	-0.32	1659	Central England	United Kingdom
5	51.47	-0.32	1659	Kew (I)	United Kingdom
77	38.72	-9	1675	Lisbon (I)	Portugal
~100	37.58	23.43	1675	Greece (I)	Greece
65	49	2.5	1676	Paris	France
15	59.9	17.6	1721	Uppsala	Sweden
4	65.5	24.08	1737	Tornio	Finland
2	59.97	30.3	1743	Petersburg	Russia
59	60.52	22.27	1748	Turku	Finland
73	55.72	13.22	1752	Lund	Sweden
405	46.2	6.2	1752	Geneva	Switzerland
318	47.6	7.6	1754	Basel	Switzerland
44	59.4	18.1	1756	Stockholm	Sweden
109	50.1	8.7	1757	Frankfurt	Germany
103	45.5	9.2	1762	Milan	Italy
134	55.92	-3.18	1763	Edinburgh	United Kingdom
383	48.05	14.13	1766	Kremsmünster	Austria
5	55.7	12.6	1767	Copenhagen	Denmark
380	50.1	14.3	1770	Prague	Czech Republic
203	48.23	21.8	1775	Vienna	Austria
156	54.63	25.28	1776	Vilnius	Lithuania
106	52.1	21	1778	Warszawa	Poland
51	52.5	13.3	1779	Berlin–Tempelhof	Germany
51	52.5	13.3	1779	Berlin	Germany
130	47.5	19	1779	Budapest	Hungary
215	50.93	11.58	1779	Jena	Germany
112	49.1	8.4	1780	Karlsruhe	Germany
268	49.8	9.95	1780	Würzburg	Germany
529	48.1	11.5	1780	München	Germany
977	47.8	11	1780	Hohenpeissenberg	Germany
120	51.1	16.9	1791	Wroclaw	Poland
236	50	20	1791	Cracow	Poland
314	48.8	9.2	1791	Stuttgart	Germany
~100	51	4	1793	Central Belgium	Belgium
6	56.97	24.07	1794	Riga	Latvia
577	47.27	11.4	1797	Innsbruck	Austria
3	53.1	8.1	1802	Bremen	Germany
~5–57	66	24	1802	Tornedalen	Sweden
447	46.65	14.33	1812	Klagenfurt	Austria
12	60.38	5.33	1815	Bergen	Norway
17	63.5	10.9	1817	Trondheim	Norway
2472	45.52	7.1	1817	Grand-St–Bernhard	Switzerland
17	65.08	-22.73	1822	Stykkisholmur	Iceland
230	51.05	13.75	1827	Dresden	Germany

## APPENDIX 1. (Continued)

H (m)	Lat (N+)	Lon (E+)	Start year	Station name	Country
51	60.3	25	1829	Helsinki	Finland
14	70.37	31.1	1830	Vardo	Norway
100	50.8	4.4	1833	Uccle	Belgium
115	54.6	-6	1833	Belfast	United Kingdom
72	51.9	8.38	1834	Gütersloh	Germany
569	47.4	8.6	1835	Zürich	Switzerland
369	47.07	15.45	1836	Graz	Austria
116	55.78	49.18	1845	Kazan	Russia
158	58.65	49.62	1845	Kirov	Russia
3	44.4	8.9	1849	Genova	Italy
16	53.4	10	1850	Hamburg	Germany
27	47.3	-1.6	1850	Nantes	France
444	45.8	24.1	1851	Sibiu	Romania
2156	46.6	13.67	1852	Villacher Alpen	Austria
91	35.85	14.48	1853	Luqa	Malta
1081	47.1	13.12	1854	Bad Gastein	Austria
56	52.5	9.7	1855	Hannover	Germany
468	47.72	13.63	1855	Bad Ischl	Austria
82	44.4	26.1	1856	Bucharest	Romania
119	61.67	50.81	1858	Sykyvkar	Russia
108	47.48	21.63	1859	Debrecen	Hungary
809	31.8	35.2	1860	Jerusalem	Israel
107	37.97	23.72	1862	Athens	Greece
157	45.49	15.49	1862	Zagreb/Gric	Croatia
276	46	9	1863	Lugano	Switzerland
50	50.39	-4.15	1864	Plymouth	United Kingdom
1798	46.26	9.46	1864	Sils Maria i.E.	Switzerland
70	64.17	-51.75	1865	Godthab	Denmark
13	67.3	14.4	1867	Bodo	Norway
11	51.9	-10.2	1868	Valentia	Ireland
367	47.1	24.5	1870	Bistrita	Romania
400	47.5	9.73	1870	Bregenz	Austria
65	57.2	-2.1	1871	Aberdeen	United Kingdom
305	64.7	-14.4	1871	Teigar	Faroe Islands
7	64.6	40.5	1873	Archangel	Russia
9	45.2	29.7	1875	Sulina	Romania
227	47.67	23.6	1876	Baia Mare	Romania
25	36.7	3.3	1877	Dareibeida	Algeria
88	45.8	21.3	1879	Timisoara	Romania
326	46.87	15.9	1880	Bad Gleichenberg	Austria
2490	47.25	9.35	1882	Säntis	Switzerland
27	65.7	-18.08	1884	Akureyri	Iceland
520	48.62	15.2	1884	Zwettl	Austria
156	51.57	46.03	1886	Saratov	Russia
3105	47.05	12.95	1887	Sonnblick	Austria
4	40.63	22.93	1891	Thessaloniki	Greece
800	47.28	14.78	1892	Seckau	Austria

APPENDIX 2. The collection of all climatological time series (predictors, in chronological order) used for the precipitation reconstruction. Denoted are the station elevation (H) in meters, the latitude (Lat) in degrees north, the longitude (Lon) in degrees east, and the start year of the time series, the station name and finally the country. Note that the historical indices derived from documentary evidence are marked with (I) in the station name column

H (m)	Lon (N)	Lat (E+)	Year	Station name	Country
~300	~48	~11.4	1500	South Germany (I)	Germany
565	~46.5	~7.35	1500	Mittelland (I)	Switzerland
469	50	14.4	1500	Czech Republic (I)	Czech Republic
130	47.5	19	1500	Ancient Hungary (I)	Hungary
0	36.2	-5.4	1501	Southern Spain (I)	Spain
107	37.97	23.72	1675	Athens (I)	Greece
77	38.72	-9	1675	Lisbon (I)	Portugal
3	41.3	2.1	1675	Barcelona (I)	Spain
657	40.4	-3.7	1675	Madrid (I)	Spain
61	37.9	-1.2	1675	Murcia (I)	Spain
31	27.4	-5.9	1675	Sevilla (I)	Spain
5	51.47	-0.32	1675	Kew (I)	United Kingdom
65	49	2.5	1688	Paris	France
569	47.4	8.6	1708	Zürich	Switzerland
3	52.8	-0.1	1726	Podehole	United Kingdom
4	52.3	4.7	1735	Hoofdoorp	Netherlands
73	55.72	13.22	1748	Lund	Sweden
8	43.3	5.4	1749	Marseilles	France
2	59.97	30.3	1760	Petersburg	Russia
565	46.56	7.25	1760	Bern	Switzerland
103	45.5	9.2	1764	Milan	Italy
12	60.38	5.33	1765	Bergen	Norway
~50	~51	~3	1766	Central England	United Kingdom
63	51.7	-1.2	1767	Oxford	United Kingdom
15	59.9	17.6	1774	Uppsala	Sweden
112	49.1	8.4	1780	Karlsruhe	Germany
366	49.1	12.1	1781	Regensburg	Germany
134	55.92	-3.18	1785	Edinburgh	United Kingdom
78	53.35	-2.27	1786	Manchester	United Kingdom
21	55.6	-6.2	1800	Eallabus	United Kingdom
153	48.55	7.63	1803	Strasbourg	France
380	50.1	14.3	1805	Prague	Czech Republic
265	49.8	6.7	1806	Trier	Germany
29.5	36.45	-5.75	1806	San Fernando	Spain
314	48.8	9.2	1807	Stuttgart	Germany
461	48.4	10.9	1812	Augsburg	Germany
60	44.48	11.75	1813	Bologna	Italy
447	46.65	14.33	1814	Klagenfurt	Austria
320	50	11.6	1814	Bayreuth	Germany
115	54.6	-6	1819	Belfast	United Kingdom
64	52	7.6	1819	Münster	Germany
383	48.05	14.13	1820	Kremsmünster	Austria
405	46.2	6.2	1826	Geneva	Switzerland
109	50.1	8.7	1826	Frankfurt	Germany
315	51	11	1827	Erfurt	Germany
231	51.1	13.7	1828	Wahnsdorf	Germany
65	57.2	-2.1	1829	Aberdeen	United Kingdom
3	53.1	8.1	1830	Bremen	Germany

## APPENDIX 2. (Continued)

H (m)	Lon (N)	Lat (E+)	Year	Station name	Country
227	47.3	5.1	1831	Dijon	France
100	50.8	4.4	1833	Uccle	Belgium
49	54.13	-8.47	1833	Markree	Ireland
91	50.9	-0.8	1834	Chilgrove	United Kingdom
152	43.6	1.4	1835	Toulouse	France
77	38.72	-9	1835	Lisbon	Portugal
51	50.1	-5.1	1835	Fallmouth	United Kingdom
27	47.3	-1.6	1835	Nantes	France
154	51.8	-8.5	1836	Cork	Ireland
71	53.4	-6.2	1837	Dublin	Ireland
72	51.9	8.4	1837	Guetersloh	Germany
704	36.3	6.6	1838	Constantine	Algeria
62	54.3	-6.6	1840	Armagh	Ireland
15	53.8	10.7	1840	Lübeck	Germany
130	47.5	19	1841	Budapest	Hungary
91	35.85	14.48	1841	Luqa	Malta
106	52.1	21	1841	Warszawa	Poland
8	45.7	13.8	1841	Trieste	Italy
217	48.7	6.2	1841	Nancy	France
201	45.7	4.8	1841	Lyon	France
4	57.5	-4.2	1841	Inverness	United Kingdom
203	48.23	21.8	1841	Vienna	Austria
122	52.3	-0.8	1841	Althorp	United Kingdom
51	44.8	-0.7	1842	Bordeaux	France
42	52.3	-7.1	1843	Waterford	Ireland
14	52.92	4.78	1844	De Kooy	Netherlands
109	51.75	55.1	1844	Orenburg	Russia
427	41.68	44.95	1844	Tbilisi	Georgia
70	53.08	-7.88	1845	Birr	United Kingdom
809	31.8	35.2	1846	Jerusalem	Israel
2	53.7	-0.3	1847	Hull	United Kingdom
113	52.7	-2.3	1847	Shifnal	United Kingdom
42	46.48	30.63	1847	Odessa	Ukraine
1	53.2	14.6	1848	Szczecin	Poland
12	52.2	0.1	1848	Cambridge	United Kingdom
51	52.5	13.3	1848	Berlin	Germany
529	48.1	11.5	1848	München	Germany
80	51.6	13	1848	Torgau	Germany
2	52.1	5.18	1849	De Bilt	Netherlands
33	51.7	-5.1	1849	Pembroke	United Kingdom
48	42.7	2.9	1850	Perpignan	France
36	58.45	-3.08	1850	Wick	United Kingdom
444	45.8	24.1	1851	Sibiu	Romania
5	53.2	7.1	1851	Emden	Germany
4	54.3	10.1	1851	Kiel	Germany
3	64.58	40.5	1852	Arkhangelsk	Russia
367	47.1	24.5	1853	Bistrita	Romania
16	53.4	10	1853	Hamburg	Germany
176	55.75	37.57	1853	Moscow	Russia
379	49.6	6.1	1854	Luxembourg	Luxembourg

(continued overleaf)

APPENDIX 2. (*Continued*)

H (m)	Lon (N)	Lat (E+)	Year	Station name	Country
116	55.78	49.18	1855	Kazan	Russia
5	41.9	8.8	1856	Ajaccio	France
56	52.5	9.7	1856	Hannover	Germany
176	50.4	30.45	1856	Kiev	Ukraine
17	65.08	-22.73	1857	Stykkisholmur	Iceland
339	57	-3.4	1857	Braemar	United Kingdom
120	51.1	16.9	1859	Wroclaw	Poland
25	36.7	3.3	1859	Dareibeida	Algeria
9	51.5	-3.2	1859	Cardiff	United Kingdom
1081	47.1	13.12	1859	Bad Gastein	Austria
468	47.72	13.63	1859	Bad Ischl	Austria
657	40.4	-3.7	1860	Madrid	Spain
5	65.82	24.13	1860	Happaranda	Sweden
276	46	9	1861	Lugano	Switzerland
11	51.9	-10.2	1861	Valentia	Ireland
42	57.67	18.33	1861	Visby	Sweden
6	52.7	-8.9	1861	Shannon	Ireland
46	59.35	13.47	1861	Karlstad	Sweden
34	54.2	16.2	1861	Koszalin	Poland
157	45.49	15.49	1862	Zagreb/Gric	Croatia
376	63.18	14.48	1862	Oestersund	Sweden
69	41.23	-8.68	1863	Oporto	Portugal
20	43.1	16.27	1864	Hvar	Croatia
1798	46.26	9.46	1864	Sils Maria i.E.	Switzerland
318	47.6	7.6	1864	Basel	Switzerland
1073	47.03	6.59	1864	Chaumont	Switzerland
1035	46.49	8.25	1864	Engelberg	Switzerland
482	46.22	7.33	1864	Sion	Switzerland
2472	45.52	7.1	1864	Grand-St.-Bernhard	Switzerland
82	44.4	26.1	1865	Bucharest	Romania
67	37.7	-25.7	1865	Pontadel	Portugal
369	47.07	15.45	1865	Graz	Austria
428	47.8	13.03	1865	Salzburg	Austria
141	40.2	-8.4	1866	Coimbra	Portugal
94	59.95	10.72	1866	Oslo	Norway
577	47.27	11.4	1866	Innsbruck	Austria
43	62.02	-6.77	1868	Torshavn	Faroe Islands
9	45.2	29.7	1869	Sulina	Romania
13	67.3	14.4	1869	Bodo	Norway
309	38.57	-7.9	1870	Evora	Portugal
107	37.97	23.72	1871	Athens	Greece
88	45.8	21.3	1873	Timisoara	Romania
15	58.22	-6.32	1873	Stornoway	United Kingdom
400	47.5	9.73	1875	Bregenz	Austria
81	32.67	13.15	1879	Tripolis	Libia
327	68.4	22.48	1879	Karesuanda	Sweden
985	46.29	7.09	1879	Chateau	Switzerland
326	46.87	15.9	1880	Bad Gleichenberg	Austria
77	44.6	22.6	1883	Severin	Romania
520	48.62	15.2	1884	Zwettl	Austria

## APPENDIX 2. (Continued)

H (m)	Lon (N)	Lat (E+)	Year	Station name	Country
102	54.8	-1.6	1886	Durham	United Kingdom
24	33.9	35.5	1888	Beirut	Lebanon
82	60.13	-1.18	1890	Lerwick	United Kingdom
20	55.37	-7.33	1890	Malin	Ireland
66	58.3	26.72	1891	Tartu	Estonia
6	56.97	24.07	1891	Riga	Latvia
20	54.7	20.62	1891	Kaliningrad	Russia
800	47.28	14.78	1892	Seckau	Austria
54	49.2	-2.1	1894	Maison/St.Louis	United Kingdom

## REFERENCES

- Auer I, Böhm R, Maugeri M. 2000. A new long-term gridded precipitation data-set for the Alps and its application for MAP and ALPCLIM. *Journal for Physics and Chemistry of the Earth (B)* **26**: 421–424.
- Auer I, Böhm R, Schöner W. 2001a. Long climatic time series from Austria. *History and Climate – Memories of the future?* Jones PD, Ogilvie AEJ, Davies TD, Briffa KR (eds). Kluwer Academic: New York, 125–151.
- Auer I, Böhm R, Brunetti M, Maugeri M, Nanni T, Schöner W. 2001b. Austrian long-term climate 1767–2000. *Multiple Instrumental Climate Time Series from Central Europe (ALOCCLIM)*. *österreich. Beiträge zu Meteorologie und Geophysik*, vol. 25, ZAMG: Vienna.
- Auer I, Böhm R, Jurkovic A, Orklik A, Potzmann R, Schöner W, Ungersböck M, Brunetti M, Nanni T, Maugeri M, Briffa K, Jones P, Efthymiadis D, Mestre O, Moisselin JM, Begert M, Brázdil R, Bochnice O, Cegnar T, Gajic-Capka M, Zaninovic K, Majstorovic Z, Szalai S, Szentimrey T, Mercalli L. 2005. A new instrumental precipitation dataset for the greater Alpine region for the period 1800–2002. *International Journal of Climatology* **25**: 139–166.
- Begert M, Schlegel T, Kirchhofer W. 2005. Homogeneous temperature and precipitation series of Switzerland from 1864 to 2000. *International Journal of Climatology* **25**: 65–80.
- Bauer E, Claussen M, Brovkin V, Huenerbein A. 2003. Assessing climate forcings of the Earth system for the past millennium. *Geophysical Research Letters* **30**: 1276. DOI:10.1029/2002GL016639.
- Beniston M, Jungo P. 2002. Shifts in the distribution of pressure, temperature and moisture and changes in the typical weather patterns in the Alpine region in response to the behavior of the North Atlantic Oscillation. *Theoretical and Applied Climatology* **71**: 29–42.
- Beniston M, Rebetez M, Giorgi F, Marinucci MR. 1994. An analysis of regional climate change in Switzerland. *Theoretical and Applied Climatology* **49**: 135–159.
- Böhm R, Auer I, Brunetti M, Maugeri M, Nanni T, Schöner W. 2001. Regional temperature variability in the European Alps: 1760–1998 from homogenized instrumental time series. *International Journal of Climatology* **21**: 1779–1801.
- Bradley RS, Jones PD. 1993. “Little Ice Age” summer temperature variations: their nature and relevance to recent global warming trends. *The Holocene* **3**: 367–376.
- Brázdil R, Pfister C, Wanner H, von Storch H, Luterbacher J. 2005. Historical climatology in Europe – the state of the art. *Climatic Change* **70**: 363–430.
- Briffa KR, Jones PD, Schweingruber FH, Osborn TJ. 1998. Influence of volcanic eruptions on Northern Hemisphere summer temperatures over 600 years. *Nature* **393**: 450–455.
- Briffa KR, Osborn TJ, Schweingruber FH. 2004. Large-scale temperature inferences from tree rings: a review. *Global and Planetary Change* **40**: 11–26.
- Briffa KR, Osborn TJ, Schweingruber FH, Jones PD, Shiyatov SG, Vaganov EA. 2002. Tree-ring width and density data around the Northern Hemisphere: part 1, local and regional climate signals. *Holocene* **12**: 737–758.
- Briffa KR, Osborn TJ, Schweingruber FH, Harris IC, Jones PD, Shiyatov SG, Vaganov EA. 2001. Low-frequency temperature variations from a northern tree ring density network. *Journal of Geophysical Research* **106**: 2929–2941.
- Büntgen U, Esper J, Frank DC, Nicolussi K, Schmidhalter M. 2005. A 1052-year tree-ring proxy for Alpine summer temperatures. *Climate Dynamics* **24**: DOI: 10.1007/s00382-005-0028-1.
- Casty C, Handorf D, Raible CC, Gonzalez-Rouco FJ, Weisheimer A, Xoplaki E, Luterbacher J, Dethloff K, Wanner H. 2005a. Recurrent climate winter regimes in reconstructed and modelled 500 hPa geopotential height fields over the North Atlantic/European sector 1659–1990. *Climate Dynamics* **24**: 809–822 DOI: 10.1007/s00382-004-0496-8.
- Casty C, Handorf D, Sempy M. 2005b. Combined Climate winter regimes over the North Atlantic/European sector 1760–2000. *Geophysical Research Letters* **32**: DOI: 10.1029/2005GLO22431.
- Chuine I, Yiou P, Viovy N, Seguin B, Daux V, Ladurie EL. 2004. Historical phenology: Grape ripening as a past climate indicator. *Nature* **432**: 289–290.
- Cook ER, Briffa KR, Jones PD. 1994. Spatial regression methods in dendroclimatology – a review and comparison of two techniques. *International Journal of Climatology* **14**: 379–402.
- Cook ER, D’Arrigo RD, Mann ME. 2002. A well-verified, multiproxy reconstruction of the Winter North Atlantic Oscillation Index since A.D. 1400. *Journal of Climate* **15**: 1754–1764.
- Cook ER, Esper J, D’Arrigo RD. 2004. Extra-tropical Northern Hemisphere land temperature variability over the past 1000 years. *Quaternary Science Reviews* **23**: 2063–2074.
- Crowley TJ. 2000. Causes of climate change over the past 1000 years. *Science* **289**: 270–277.

- Crowley TJ, Lowery TS. 2000. How warm was the medieval warm period? A comment on 'Man-made *versus* natural climate change'. *Ambio* **39**: 51–54.
- Czaja A, Frankignoul C. 1999. Influence of the North Atlantic SST on the atmospheric circulation. *Geophysical Research Letters* **26**: 2969–2972.
- Davis RE, Hayden BP, Gay DA, Phillips WL, Jones GV. 1997. The North Atlantic subtropical anticyclone. *Journal of Climate* **10**: 728–744.
- Esper J, Cook ER, Schweingruber FH. 2002. Low-frequency signals in long tree-ring chronologies for reconstructing past temperature variability. *Science* **295**: 2250–2253.
- Folland CK, Rayner NA, Brown SJ, Smith TM, Shen SSP, Parker DE, Macadam I, Jones PD, Jones RN, Nicholls N, Sexton DMH. 2001. Global temperature change and its uncertainties since 1861. *Geophysical Research Letters* **28**: 2621–2624.
- Frank D, Esper J. 2005. Temperature reconstructions and comparisons with instrumental data from a tree-ring network for the European Alps. *International Journal of Climatology* in press.
- Frei C, Schär C. 1998. A precipitation climatology of the Alps from high-resolution rain-gauge observations. *International Journal of Climatology* **18**: 873–900.
- Gerber S, Joos F, Brügger P, Stocker TF, Mann ME, Sitch S, Scholze M. 2003. Constraining temperature variations over the last millennium by comparing simulated and observed atmospheric CO<sub>2</sub>. *Climate Dynamics* **20**: 281–299.
- Gershunov A, Schneider N, Barnett T. 2001. Low-frequency modulation of the ENSO-Indian Monsoon rainfall relationship: signal or noise? *Journal of Climate* **14**: 2486–2492.
- Glaser R. 2001. *Klimageschichte Mitteleuropas. 1000 Jahre Wetter, Klima, Katastrophen*, Primus: Darmstadt.
- Glaser R, Brázdil R, Pfister C, Dobrovolny P, Barriendos Valle M, Bokwa A, Camuffo D, Kotyza O, Limanowka D, Racz L, Rodrigo FS. 1999. Seasonal temperature and precipitation fluctuations in selected parts of Europe during the sixteenth century. *Climatic Change* **43**: 169–200.
- González-Rouco JF, von Storch H, Zorita E. 2003. Deep soil temperature as a proxy for surface air-temperature in a coupled model simulation of the last thousand years. *Geophysical Research Letters* **30**: DOI: 10.1029/2003GL018264.
- Goose H, Crowley TJ, Zorita E, Ammann CM, Renssen H, Driesschaert E. 2005a. Modelling the climate of the last millennium: what causes the differences between simulations? *Geophysical Research Letters* **32**: DOI: 10.1029/2003GL018264.
- Goose H, Renssen H, Timmermann A, Bradley RS. 2005b. Internal and forced climate variability during the last millennium: a model-data comparison using ensemble simulations. *Quaternary Science Reviews* **24**: 1345–1360.
- Guiot J, Nicault A, Rathgeber C, Edouard JL, Guibal F, Pichard G, Till C. 2005. The last millennium summer temperature variations in Western Europe as based on proxy data. *The Holocene* **15**: 489–500.
- Gyalistras D. 2003. Development and validation of a high-resolution monthly gridded temperature and precipitation data set for Switzerland (1951–2000). *Climate Research* **25**: 55–83.
- Hansen J, Ruedy R, Glasco J, Sato M. 1999. GISS analysis of surface temperature change. *Journal of Geophysical Research* **104**: 30 997–31 022.
- Hansen J, Ruedy R, Sato M, Imhoff M, Lawrence W, Easterling D, Peterson T, Karl T. 2001. A closer look at United States and global surface temperature change. *Journal of Geophysical Research* **106**: 23 947–23 963.
- Huang S. 2004. Merging information from different resources for new insights into climate change in the past and future. *Geophysical Research Letters* **31**: DOI: 10.1029/2004GL019781.
- Hurrell JW, van Loon H. 1997. Decadal variations in climate associated with the North Atlantic oscillation. *Climatic Change* **36**: 301–326.
- Hurrell JW, Kushnir Y, Ottersen G, Visbeck M (eds). 2003. *The North Atlantic Oscillation: Climate Significance and Environmental Impact*, *Geophysical Monograph Series 134*: American Geophysical Union, Washington, DC.
- IPCC. 2001. *Climate Change 2001: The Scientific Basis*, Houghton JT, Ding Y, Griggs DJ, Noguer M, van der Linden PJ, Dai X, Maskell K, Johnson CA (eds). Cambridge University Press: Cambridge, UK.
- Jacobeit J, Wanner H, Koslowski G, Gudd M. 1999. European surface pressure patterns for months with outstanding climatic anomalies during the sixteenth century. *Climatic Change* **43**: 201–221.
- Jacobeit J, Wanner H, Luterbacher J, Beck C, Phillip A, Sturm K. 2003. Atmospheric circulation variability in the North-Atlantic-European area since the mid-seventeenth century. *Climate Dynamics* **20**: 341–352.
- Jones PD, Mann ME. 2004. Climate over past millennia. *Reviews of Geophysics* **42**: RG2002. DOI: 10.1029/2003RG000143.
- Jones PD, Osborn TJ, Briffa KR. 2001. The evolution of climate over the last millennium. *Science* **292**: 662–666.
- Jones PD, Briffa KR, Barnett TP, Tett SFB. 1998. High-resolution palaeoclimatic records for the last Millennium: Interpretation, integration and comparison with general circulation model control-run temperatures. *Holocene* **8**: 455–471.
- Jones PD, New M, Parker DE, Martin S, Rigor IG. 1999. Surface air temperatures and its changes over the past 150 years. *Reviews on Geophysics* **37**: 173–199.
- Kettle H, Thompson R. 2004. Statistical downscaling in European mountains: verification of reconstructed air temperature. *Climate Research* **26**: 97–112.
- Koppe C, Kovats RS, Jendritzky G, Menne B. 2004. Heat-waves: impacts and responses. In *Health and Global Environmental Change Series*, vol. 2, WHO Regional Office for Europe: Copenhagen.
- Kovats RS, Koppe C. 2005. Heatwaves: past and future impacts. *Integration of Public Health with Adaptation to Climate Change: Lessons Learned and New Directions*, Ebi K, Burton I, Smith J. (eds) Lisse, Swets & Zeitlinger: in press.
- Kovats RS, Hajat S, Wilkinson P. 2004. Contrasting patterns of mortality and hospital admissions during hot weather and heat waves in Greater London, UK. *Occupational & Environmental Medicine* **61**: 893–898.
- Luterbacher J, Luterbacher J, Rickli R, Tinguely C, Xoplaki E, Schüpbach E, Dietrich D, Hüsler J, Ambühl M, Pfister C, Beeli P, Dietrich U, Dannecker A, Davies TD, Jones PD, Slonosky V, Ogilvie AEJ, Maheras P, Kolyva-Machera F, Martin-Vide J, Barriendos M, Alcoforado MJ, Nunez F, Jónsson T, Glaser R, Jacobeit J, Beck C, Phillip A, Beyer U, Kaas E, Schmith T, Barring L, Jónsson P, Rácz L, Wanner H. 2000. Reconstruction of monthly mean sea level pressure over Europe for the late maunder minimum period (1675–1715). *International Journal of Climatology* **20**: 1049–1066.

- Luterbacher J, Schmutz C, Gyalistras D, Xoplaki E, Wanner H. 1999. Reconstruction of monthly NAO and EU indices back to A.D. 1675. *Geophysical Research Letters* **26**: 2745–2748.
- Luterbacher J, Dietrich D, Xoplaki E, Grosjean M, Wanner H. 2004. European seasonal and annual temperature variability, trends and extremes since 1500. *Science* **303**: 1499–1503.
- Luterbacher J, Rickli R, Xoplaki E, Tinguely C, Beck C, Pfister C, Wanner H. 2001. The late maunder minimum (1675–1715) – a key period for studying decadal scale climatic change in Europe. *Climatic Change* **49**: 441–462.
- Luterbacher J, Xoplaki E, Dietrich D, Rickli R, Jacobeit J, Beck C, Gyalistras D, Schmutz C, Wanner H. 2002a. Reconstruction of sea level pressure fields over the Eastern North Atlantic and Europe back to 1500. *Climate Dynamics* **18**: 545–561.
- Luterbacher J, Xoplaki E, Dietrich D, Jones PD, Davies TD, Porties D, Gonzalez-Rouco JF, von Storch H, Gyalistras D, Casty C, Wanner H. 2002b. Extending North Atlantic oscillation reconstructions back to 1500. *Atmospheric Science Letters* **2**: 114–124.
- Mann ME, Bradley RS, Hughes MK. 1998. Global-scale temperature patterns and climate forcing over the past six centuries. *Nature* **392**: 779–787.
- Mann ME, Bradley RS, Hughes MK. 1999. Northern hemisphere temperatures during the past millennium: inferences, uncertainties, and limitations. *Geophysical Research Letters* **26**: 759–762.
- Mann ME, Gille E, Bradley RS, Hughes MK, Overpeck JT, Keimig FT, Gross W. 2000. Global temperature patterns in past centuries: an interactive presentation. *Earth Interactions* **4**: 1–29.
- Menzel A. 2005. A 500 year pheno-climatological view on the 2003 heatwave in Europe assessed by grape harvest dates. *Meteorologische Zeitschrift* **14**: 75–77.
- Mitchell TD, Carter TR, Jones PD, Hulme M, New M. 2004. *A Comprehensive Set of High-resolution Grids of Monthly Climate for Europe and the Globe: The Observed Record (1901–2000) and 16 Scenarios (2001–2100)*. Working Paper 55, Tyndall Center for Climate Change.
- Moberg AD, Sonechkin M, Holmgren K, Datsenko NM, Karlen W. 2005. Highly variable Northern Hemisphere temperatures reconstructed from low- and high-resolution proxy data. *Nature* **433**: 613–617.
- New ME, Hulme M, Jones PD. 2000. Representing twentieth-century space-time climate variability. Part II: development of 1901–1996 monthly grids of terrestrial surface climate. *Journal of Climate* **13**: 2217–2238.
- Oerlemans JH. 2005. Extracting a climate signal from 169 glacier records. *Science* **308**: 675–677 DOI: 10.1126/science.1107046.
- Overpeck J, Hughen K, Hardy D, Bradley RS, Case R, Douglas M, Finney B, Gajewski K, Jacoby K, Jennings A, Lamoureux S, Lasca A, Moore GMJ, Retelle M, Smith S, Wolfe A, Zielinski G. 1997. Arctic environmental change of the last four centuries. *Science* **278**: 1251–1256.
- Pal JS, Giorgi F, Bi X. 2004. Consistency of recent European summer precipitation trends and extremes with future regional climate projections. *Geophysical Research Letters* **31**: L13202. DOI: 10.1029/2004GL019836.
- Palmer TN, Sun Z. 1985. A modelling and observational study of the relationship between sea surface temperature in the north-west Atlantic and the atmospheric general circulation. *Quarterly Journal of the Royal Meteorological Society* **111**: 947–975.
- Pauling A, Luterbacher J, Casty C, Wanner H. 2005. 500 years of gridded high-resolution precipitation reconstructions over Europe and the connection to large-scale circulation. *Climate Dynamics* revised.
- Pfister C. 1999. *Wetternachhersage*. Haupt: Bern.
- Pfister C. 1992. Monthly temperature and precipitation in Central Europe 1525–1979: quantifying documentary evidence on weather and its effects. *Climate since A.D. 1500*, Bradley RS, Jones PD (eds). Routledge: London.
- Pollack HN, Smerdon JE. 2004. Borehole climate reconstructions: spatial structure and hemispheric averages. *Journal of Geophysical Research* **109**: DOI: 10.1029/2003JD004163.
- Portis DH, Walsh JE, El Hamly M, Lamb PJ. 2001. Seasonality of the North Atlantic oscillation. *Journal of Climate* **14**: 2069–2078.
- Rebetez M. 2004. Summer 2003 maximum and minimum daily temperatures over a 3300 m altitudinal range in the Alps. *Climate Research* **27**: 45–50.
- Rutherford S, Mann ME, Delworth TL, Stouffer R. 2003. Climate field reconstruction under stationary and nonstationary forcing. *Journal of Climate* **16**: 462–479.
- Rutherford SD, Mann ME, Osborn TJ, Bradley RS, Briffa KR, Hughes MK, Jones PD. 2005. Proxy-based Northern Hemisphere surface temperature reconstructions: sensitivity of methodology, predictor network, target season and target domain. *Journal of Climate* **18**: 2308–2329.
- Schär C, Vidale PL, Lüthi D, Frei C, Häberli C, Liniger MA, Appenzeller C. 2004. The role of increasing temperature variability in European summer heatwaves. *Nature* **427**: 332–336.
- Scherhag R. 1948. *Wetteranalyse und Wetterprognose*, Springer: Berlin.
- Schmidli J, Frei C, Schär C. 2001. Reconstruction of mesoscale precipitation fields from sparse observations in complex terrain. *Journal of Climate* **14**: 3289–3306.
- Schmidli J, Schmutz C, Frei C, Wanner H, Schär C. 2002. Mesoscale precipitation variability in the region of the European Alps during the 20th century. *International Journal of Climatology* **22**: 1049–1074.
- Schmutz C, Luterbacher J, Gyalistras D, Xoplaki E, Wanner H. 2000. Can we trust proxy-based NAO index reconstructions. *Geophysical Research Letters* **27**: 1135–1138.
- Schönwiese CD, Staeger T, Tromel S. 2004. The hot summer 2003 in Germany. Some preliminary results of a statistical time series analysis. *Meteorologische Zeitschrift* **13**: 323–327.
- Slonosky VC, Jones PD, Davies TD. 2001. Atmospheric circulation and surface temperature in Europe from the 18th century to 1995. *International Journal of Climatology* **21**: 63–75.
- Stéphan F, Ghiglione S, Decailliot F, Yakhou L, Duvaldestin P, Legrand P. 2005. Effect of excessive environmental heat on core temperature in critically ill patients. An observational study during the 2003 European heat wave. *British Journal of Anaesthesia* **94**: 39–45.
- Stott PA, Stone DA, Allen MR. 2004. Human contribution to the European heatwave of 2003. *Nature* **432**: 610–614.
- Valleron AJ, Boumendil A. 2004. Epidemiology and heat waves: analysis of the 2003 episode in France. *Comptes Rendus Biologies* **327**: 1125–1141.
- von Storch H, Zwiers FW. 2001. *Statistical analysis in Climate research.*, Cambridge University Press: Cambridge.

- von Storch H, Zorita E, Jones J, Dimitriev Y, González-Rouco JF, Tett S. 2004. Reconstructing past climate from noisy data. *Science* **306**: 679–682.
- Wanner H, Luterbacher J. 2002. The LOTRED approach – a first step towards a “paleoreanalysis” for Europe. *Pages News* **10**: 9–11.
- Wanner H, Rickli R, Salvisberg E, Schmutz C, Schüepf M. 1997. Global climate change and variability and its influence on Alpine climate – concepts and observations. *Theoretical and Applied Climatology* **58**: 221–243.
- Wanner H, Brönnimann S, Casty C, Gyalistras D, Luterbacher J, Schmutz C, Stephenson DB, Xoplaki E. 2001. North Atlantic oscillation – concepts and studies. *Surveys in Geophysics* **22**: 321–382.
- Wilks DS. 1995. *Statistical Methods in the Atmospheric Sciences: an Introduction*, Academic Press: London.
- Wilson RJS, Luckman BH, Esper J. 2005. A 500 year dendroclimatic reconstruction of spring-summer precipitation from the lower Bavarian forest region, Germany. *International Journal of Climatology* **25**: 611–630.
- Xie P, Arkin PA. 1997. Global precipitation: a 17-year monthly analysis based on gauge observations, satellite estimates, and numerical model outputs. *Bulletin of the American Meteorological Society* **78**: 2539–2558.
- Xoplaki E, Luterbacher J, Paeth H, Dietrich D, Steiner N, Grosjean M, Wanner H. 2005. European spring and autumn temperature variability and change of extremes over the last half millenium. *Geophysical Research Letters* **32**: DOI: 10.29/2005GLO23424.